ARL-TR-7694 • MAY 2016

US Army Research Laboratory

Finsler-Geometric Continuum Mechanics

by John D Clayton

NOTICES

Disclaimers

The findings in this report are not to be construed as an official Department of the Army position unless so designated by other authorized documents.

Citation of manufacturer's or trade names does not constitute an official endorsement or approval of the use thereof.

Destroy this report when it is no longer needed. Do not return it to the originator.

ARL-TR-7694 ● MAY 2016

US Army Research Laboratory

Finsler-Geometric Continuum Mechanics

by John D Clayton
Weapons and Materials Research Directorate, ARL

REPORT DOCUMENTATION PAGE

Form Approved
OMB No. 0704-0188

PLEASE DO NOT RETURN YOUR FORM TO THE ABOVE ADDRESS.

1. REPORT DATE *(DD-MM-YYYY)*	2. REPORT TYPE	3. DATES COVERED (From - To)
May 2016	Final	October 2015–May 2016

4. TITLE AND SUBTITLE
Finsler-Geometric Continuum Mechanics

5a. CONTRACT NUMBER

5b. GRANT NUMBER

5c. PROGRAM ELEMENT NUMBER

6. AUTHOR(S)
John D Clayton

5d. PROJECT NUMBER
AH80

5e. TASK NUMBER

5f. WORK UNIT NUMBER

7. PERFORMING ORGANIZATION NAME(S) AND ADDRESS(ES)
US Army Research Laboratory
ATTN: RDRL-WMP-C
Aberdeen Proving Ground, MD 21005-5066

8. PERFORMING ORGANIZATION REPORT NUMBER
ARL-TR-7694

9. SPONSORING/MONITORING AGENCY NAME(S) AND ADDRESS(ES)

10. SPONSOR/MONITOR'S ACRONYM(S)

11. SPONSOR/MONITOR'S REPORT NUMBER(S)

12. DISTRIBUTION/AVAILABILITY STATEMENT
Approved for public release; distribution is unlimited.

13. SUPPLEMENTARY NOTES
primary author's email: <johnclay@cims.nyu.edu>.

14. ABSTRACT
Concepts from Finsler differential geometry are applied toward a theory of deformable continua with microstructure. The general model accounts for finite strains, nonlinear elasticity, and various kinds of structural defects in a solid body. The general kinematic structure of the theory includes macroscopic and microscopic displacement fields (i.e., a multiscale theory) whereby the latter are represented mathematically by the director vector of pseudo-Finsler space, not necessarily of unit magnitude. Variational methods are applied to derive Euler-Lagrange equations for static equilibrium and Neumann boundary conditions. The theory is specialized in turn to physical problems of tensile fracture, shear localization, and cavitation in solid bodies. The pseudo-Finsler approach is demonstrated to be more general than classical approaches and can reproduce phase field solutions when certain simplifying assumptions are imposed. Upon invoking a conformal or Weyl-type transformation of the fundamental tensor, analytical and numerical solutions of representative example problems offer new physical insight into coupling of microscopic dilatation with fracture or slip.

15. SUBJECT TERMS
continuum physics, solid mechanics, differential geometry, nonlinear elasticity, fracture, shear localization, phase field

16. SECURITY CLASSIFICATION OF:			17. LIMITATION OF ABSTRACT	18. NUMBER OF PAGES	19a. NAME OF RESPONSIBLE PERSON
a. REPORT	b. ABSTRACT	c. THIS PAGE			John D Clayton
Unclassified	Unclassified	Unclassified	UU	72	19b. TELEPHONE NUMBER (Include area code) 410-278-6146

Contents

List of Figures

List of Tables

Acknowledgments

This report was written while I served as a visiting research fellow at the Courant Institute of Mathematical Sciences (CIMS) in New York, NY. I acknowledge the courtesy of Prof Robert (Bob) Kohn for facilitating and hosting this sabbatical visit at CIMS in 2016. I also thank academic faculty and scholars at CIMS and at Columbia University (New York, NY) in the departments of applied mathematics, physics, and engineering mechanics for offering suggestions regarding my work on Finsler-geometric continuum physics following technical seminars at each institution during the Spring semester of 2016. The present US Army Research Laboratory technical report, besides presenting initial/exploratory research on the title topic, partially fulfills an institutional requirement regarding documentation of work performed during my sabbatical stay.

INTENTIONALLY LEFT BLANK.

1. Introduction

In Finsler geometry, each point on the base manifold can be envisioned as endowed with a vector of coordinates denoting its position from the origin and a director vector, also referred to herein as an internal state vector, that may be independent of position. Geometric objects such as metric tensors, connections, and derived quantities (torsion, curvature, and so forth) may in turn depend on position and direction or internal state. This generality is in contrast to classical Riemannian geometry, wherein the ultimate dependence of such objects is on position alone. Indeed, Finsler geometry encompasses certain geometries of Riemann, Minkowski, and Weyl as special cases. Its generality has resulted in widespread posited field-theoretical descriptions in nearly all branches of physics: general relativity,[1] gravitation,[2] quantum mechanics,[3] electrodynamics,[4] heat conduction,[5] and the mechanics of solids.[6] The latter topic (i.e., continuum mechanics/physics of deformable bodies) is emphasized in the present report. In this context, fields describing the motion of material particles comprising a body must be introduced along with evolution of the internal state, specifically transformations from referential or Lagrangian coordinates and initial state vectors to spatial or Eulerian coordinates and current state vectors.

Finsler geometry is attributed by name to the doctoral work of P Finsler nearly a century ago.[7] Early fundamental contributions, including the introduction of various connections, were set forth by Cartan,[8] Chern,[9] and Rund.[10] Modern monographs include references 11–13. Of particular interest here is reference 14, since it includes a chapter devoted to applications in finite deformation of solids, albeit with content limited to kinematics alone. See also the historical review in reference 15—a paper that also advances Finsler geometry via extension of the Cartan-Clifton method of moving frames—and the recent categorization of Finsler connections in reference 16.

Applications of Finsler geometry in continuum mechanics and physics of deformable solids have been suggested, but not fully developed or realized, since the middle of the 20th century. Amari[17] developed what appears to be the first Finsler geometric theory of deformation of solids, applied specifically to ferromagnetic elastic-plastic crystals. In this theory, the internal state vector is physically linked to the spin direction of the magnetic moment, and dislocations (a fundamental line defect in crystalline solids[18,19]) are associated with a certain torsion tensor related to anholo-

nomicity[20–25] of the locally relaxed intermediate state of the crystal, following earlier classical differential-geometric treatments by Kondo[26] and the Japanese school. Kondo[27] briefly discussed possible application of Finsler geometry to describe plastic yielding. Kröner[28] and Eringen[29] suggested how Finsler geometry may be of potential use for describing mechanics of solids in the context of generalized continuum theories such as, for example, reference 30, but did not further develop or expound on these ideas. Around the same time, Ikeda[31,32] developed a theory of deformable media with close connections to Finsler space, again restricted to description of kinematics without consideration of energy functionals or equilibrium equations. Apparently, the application of (pseudo-)Finsler geometry to solid mechanics remained dormant for some 20 years after these suggestions, until the appearance of work by Bejancu,[14] followed in the next decade by contributions from Saczuk and colleagues.[6,33] (Herein, a space is designated as pseudo-Finslerian[14,16] rather than strictly Finslerian when a fundamental scalar function with requisite properties,[11] from which the metric tensor is obtained by differentiation, does not exist.) Theoretical developments again remained scarce for 15 years following, apart from some recent work on anisotropic acoustic wave propagation.[34] For a more comprehensive current literature review, see reference 35.

It is speculated that Finsler geometry, in contrast to Riemannian geometry,[36–40] has heretofore eluded popularity among mechanicians and physicists due to the apparent complexity of calculations, despite its generality and descriptive potential. Indeed, only one published paper[33] containing solutions to a boundary value problem in Finsler-geometric solid mechanics seems to exist, and these solutions were obtained numerically rather than analytically and only discussed in brief (though the somewhat obscure monograph[41] contains many more details regarding the theory and problems considered in reference 33). In the absence of solutions to physically meaningful problems, a complex new theory may offer little advantage or insight over simpler existing methods.

The purpose of this report is to initiate a new theory of mechanics of deformable solids with microstructure using concepts from Finsler geometry. Although a few aspects of the proposed theory are drawn from prior work, notably references 14 and 33, many features are introduced here for the first time. The theory is constructed with an aim toward obtaining solutions to pertinent boundary value problems in mechanics, physics, and materials science. Specifically, problems consid-

ered herein include tensile fracture of an elastic bar (see, for example, reference 42 for a recent analysis in a different multiscale context), slip localization in an elastic slab under simple shear (see, for example, reference 43 for a recent analysis via phase field theory), and cavitation (e.g., void formation and expansion) in a spherical elastic domain. The fundamental metric tensor entering the theory in these problems accounts for microscopic dilatation, which is commonplace in the fracture of crystalline rocks and minerals[44–46] as well as in the vicinity of dislocation cores in crystals.[18,47] To reflect such local volume changes, a Weyl-type rescaling (i.e., a conformal transformation) of the metric tensor is invoked.[48,49] In a novel theory of thermal stresses based on Riemannian geometry, a similar rescaling of a metric tensor on the material manifold was invoked to study isotropic nonlinear elastic solids.[50] Unlike prior theoretical and computational studies in crystal inelasticity,[51–53] the present developments do not require a multiplicative decomposition of the deformation gradient into 2 (or perhaps more) terms, but such a treatment is not precluded by the general theory and has been proposed elsewhere in a merging of continuum phase field and Finsler geometric treatments of deformation twinning in crystals.[35] Applications considered herein are also restricted to initially homogeneous bodies (e.g., single crystals or homogenized polycrystals). Not considered explicitly are spatially heterogeneous bodies, such as those with varying elastic moduli[51] or varying stress-free strains,[54] though the general theory does not preclude analysis of such problems. Though this report does not apply the theory toward problems involving phase transitions or twinning, as often studied in the context of martensite,[55] the theory developed herein could be readily applied to such problems in future work.

This report is organized as follows. Kinematics and geometry pertinent to a new pseudo-Finsler theory of continuum physics are described in Section 2, including motions at macro- and microscales, strain metrics, and differential geometric objects, such as horizontal and vertical connections. An energy functional over the domain is developed in Section 3, from which Euler-Lagrange equations yield the conservation laws of static equilibrium for incremental boundary value problems. Crucial to deriving such equations is an extension of the divergence theorem forwarded in reference 56. Application of the theory toward problems involving fracture is discussed in Section 4, including the solution of a 1-dimensional (1-D) tensile decohesion problem. Application toward problems involving slip (e.g., dislocation glide, adiabatic shear band formation, or mode II separation) is presented in Section

5. Application toward problems involving cavitation is given in Section 6. In the applications sections, links among geometric objects/parameters entering the theory and physical concepts are highlighted, and comparisons with predictions of other classical field approaches are given. Conclusions follow in Section 7.

2. Pseudo-Finsler Geometry and Kinematics

Discussed in turn are aspects of the referential (e.g., initial) configuration of the material body, the deformed configuration of the material body, and then the transformations (e.g., motions) between the 2 configurations.

2.1 Reference Configuration Geometry

The reference configuration is identified with a particular instant in time at which a deformable solid body is considered undeformed, following the usual convention of continuum physics.[19] A differential manifold $\mathfrak{M}$ of spatial dimension 3 is then physically identified with a deformable solid body embedded in ambient Euclidean 3-space. Let $X \in \mathfrak{M}$ denote a material point or material particle, and let $\{X^A\}(A = 1, 2, 3)$ denote a coordinate chart that could be assumed, in the interest of brevity, to completely cover $\mathfrak{M}$. The body manifold may be taken as simply connected herein for simplicity, though such an assumption is inessential; in fact, the theory is later applied to describe breakage, slip, and cavitation processes that may preclude simple connectivity of the body in one or more conditional states. Attached to each point is a vector $\boldsymbol{D}$, or equivalently, a chart of secondary coordinates $\{D^A\}(A = 1, 2, 3)$ is assigned that is treated as a field description of microstructure in the solid and can be associated with a second manifold $\mathfrak{U}$ of dimension 3. Herein, $\boldsymbol{D}$ need not be of unit length. Analogoulsy, one may assume for temporary convenience that $\mathfrak{U}$ is simply connected and covered by a single chart, though again this assumption is not essential. Regarding notation, dependence of a function on (X, D) implies dependence on charts $(\{X^A\}, \{D^A\})$.

Following the notation of reference 14, the description of the reference state of the body can be couched in terms of pseudo-Finsler geometry. Define $\mathcal{Z} = (\mathfrak{Z}, \Pi, \mathfrak{M}, \mathfrak{U})$ as a fiber bundle of total (pseudo-Finsler) space $\mathfrak{Z}$ (dimension 6), where $\Pi : \mathfrak{Z} \to \mathfrak{M}$ is the projection and $\mathfrak{U}$ the fiber. A chart covering $\mathfrak{Z}$ is then $\{X, D\}$. The natural or holonomic basis on $\mathfrak{Z}$ is the field of frames $\{\frac{\partial}{\partial X^A}, \frac{\partial}{\partial D^A}\}$. Coordinate transformations

from $\{X, D\}$ to another chart $\{\tilde{X}, \tilde{D}\}$ are of the Finsler form[11]

$$\tilde{X}^A = \tilde{X}^A(X^1, X^2, X^3), \qquad \tilde{D}^A(X) = Q^A_B(X) D^B. \tag{1}$$

Let $Q^A_B = \frac{\partial \tilde{X}^A}{\partial X^B}$. From the chain rule, holonomic basis vectors on $T\mathfrak{Z}$ then transform as[11,14]

$$\frac{\partial}{\partial \tilde{X}^A} = \frac{\partial X^B}{\partial \tilde{X}^A}\frac{\partial}{\partial X^B} + \frac{\partial^2 X^B}{\partial \tilde{X}^A \partial \tilde{X}^C}\tilde{D}^C \frac{\partial}{\partial D^B}, \qquad \frac{\partial}{\partial \tilde{D}^A} = \frac{\partial X^B}{\partial \tilde{X}^A}\frac{\partial}{\partial D^B}. \tag{2}$$

Let $N^A_B(X, D)$ denote nonlinear connection coefficients. Nonholonomic basis vectors, which unlike their holonomic counterparts transform as typical vectors, are

$$\frac{\delta}{\delta X^A} = \frac{\partial}{\partial X^A} - N^B_A \frac{\partial}{\partial D^B}, \qquad \delta D^A = dD^A + N^A_B dX^B. \tag{3}$$

Noting the scalar products $\langle \frac{\delta}{\delta X^B}, dX^A \rangle = \delta^A_B$ and $\langle \frac{\partial}{\partial D^B}, \delta D^A \rangle = \delta^A_B$, the set $\{\frac{\delta}{\delta X^A}, \frac{\partial}{\partial D^A}\}$ serves as a convenient local basis on $T\mathfrak{Z}$, and likewise the reciprocal set $\{dX^A, \delta D^A\}$ for $T^*\mathfrak{Z}$.[16] The Sasaki metric tensor invokes the latter:

$$\boldsymbol{G}(X, D) = G_{AB}(X, D) dX^A \otimes dX^B + G_{AB}(X, D) \delta D^A \otimes \delta D^B. \tag{4}$$

Components G_{AB} and their inverse components G^{AB} are used to lower and raise indices in the usual manner, and $G(X, D) = \det[G_{AB}(X, D)]$. Differentiation is hereafter denoted by the following condensed notation:

$$\partial_A(\cdot) = \frac{\partial(\cdot)}{\partial X^A}, \quad \bar{\partial}_A(\cdot) = \frac{\partial(\cdot)}{\partial D^A}; \qquad \delta_A(\cdot) = \frac{\delta(\cdot)}{\delta X^A} = \partial_A(\cdot) - N^B_A \bar{\partial}_B(\cdot). \tag{5}$$

Christoffel symbols of the second kind for the Levi-Civita connection on $\mathfrak{M}$ are derived in the usual way:

$$\gamma^A_{BC} = \tfrac{1}{2} G^{AD}(\partial_C G_{BD} + \partial_B G_{CD} - \partial_D G_{BC}) = G^{AD}\gamma_{BCD}. \tag{6}$$

Cartan's tensor in the reference configuration is defined as

$$C^A_{BC} = \tfrac{1}{2} G^{AD}(\bar{\partial}_C G_{BD} + \bar{\partial}_B G_{CD} - \bar{\partial}_D G_{BC}) = G^{AD} C_{BCD}. \tag{7}$$

Horizontal coefficients of the Chern-Rund and Cartan connections are defined as

$$\Gamma^A_{BC} = \tfrac{1}{2}G^{AD}(\delta_C G_{BD} + \delta_B G_{CD} - \delta_D G_{BC}) = G^{AD}\Gamma_{BCD}. \tag{8}$$

Components of the spray and derived nonlinear connection coefficents are, respectively,

$$G^A = \tfrac{1}{2}\gamma^A_{BC}D^B D^C, \qquad G^A_B = \bar{\partial}_B G^A. \tag{9}$$

Letting ∇ denote the covariant derivative, horizontal gradients of basis vectors are determined by the generic affine connection coefficients H^A_{BC} and K^A_{BC}:

$$\nabla_{\delta/\delta X^B}\frac{\delta}{\delta X^C} = H^A_{BC}\frac{\delta}{\delta X^A}, \qquad \nabla_{\delta/\delta X^B}\frac{\partial}{\partial D^C} = K^A_{BC}\frac{\partial}{\partial D^A}. \tag{10}$$

Vertical gradients are denoted by the generic connection coefficients V^A_{BC} and Y^A_{BC}:

$$\nabla_{\partial/\partial D^B}\frac{\partial}{\partial D^C} = V^A_{BC}\frac{\partial}{\partial D^A}, \qquad \nabla_{\partial/\partial D^B}\frac{\delta}{\delta X^C} = Y^A_{BC}\frac{\delta}{\delta X^A}. \tag{11}$$

Developments to this point apply for pseudo-Finsler space or Finsler space. The latter classification holds when a C^∞ fundamental scalar function $\mathfrak{L}(X, D)$ exists at every point of $\mathfrak{U} \setminus 0$, homogeneous of degree one in $\boldsymbol{D}$,[11] from which the metric tensor, spray connection coefficients, and Cartan tensor are derived, the latter with additional symmetry not necessarily present in Eq. 7:

$$\begin{aligned} G_{AB} &= \tfrac{1}{2}\bar{\partial}_A\bar{\partial}_B(\mathfrak{L}^2), \qquad C_{ABC} = \tfrac{1}{4}\bar{\partial}_A\bar{\partial}_B\bar{\partial}_C(\mathfrak{L}^2); \\ G^A_B &= \gamma^A_{BC}D^C - C^A_{BC}\gamma^C_{DE}D^D D^E = \Gamma^A_{BC}D^C. \end{aligned} \tag{12}$$

Formally, the Chern-Rund connection is defined when Eq. 12 holds and $N^A_B = G^A_B$, $H^A_{BC} = K^A_{BC} = \Gamma^A_{BC}$, and $V^A_{BC} = Y^A_{BC} = 0$; the Cartan connection is defined when Eq. 12 holds and $N^A_B = G^A_B$, $H^A_{BC} = K^A_{BC} = \Gamma^A_{BC}$, and $V^A_{BC} = Y^A_{BC} = C^A_{BC}$.[16] Let $(\cdot)_{|C}$ denote horizontal covariant differentiation in a coordinate chart $\{X^C\}$. Then when either of these connections is used, the horizontal covariant derivative of the metric tensor vanishes:

$$\begin{aligned} G_{AB|C} &= \delta_C G_{AB} - \Gamma^D_{CA}G_{DB} - \Gamma^D_{CB}G_{DA} \\ &= \partial_C G_{AB} - N^D_C\bar{\partial}_D G_{AB} - \Gamma^D_{CA}G_{DB} - \Gamma^D_{CB}G_{DA} = 0. \end{aligned} \tag{13}$$

A (pseudo)-Finsler space degenerates to a Riemannian space when $G_{AB}(X, D) \to$

$G_{AB}(X)$, and to a locally Minkowskian space when $\mathfrak{L}(X, D) \to \mathfrak{L}(D)$.[16]

Let d$\boldsymbol{X}$ denote a differential line element on $\mathfrak{M}$, and let d$\boldsymbol{D}$ denote a corresponding element on $\mathfrak{U}$, both with components referred to the nonholonomic basis. Squared lengths of these elements with respect to Eq. 4 are

$$|\mathrm{d}\boldsymbol{X}|^2 = \langle \mathrm{d}\boldsymbol{X}, \boldsymbol{G}\mathrm{d}\boldsymbol{X}\rangle = G_{AB}\mathrm{d}X^A\mathrm{d}X^B, \qquad |\mathrm{d}\boldsymbol{D}|^2 = \langle \mathrm{d}\boldsymbol{D}, \boldsymbol{G}\mathrm{d}\boldsymbol{D}\rangle = G_{AB}\mathrm{d}D^A\mathrm{d}D^B. \tag{14}$$

The traditional scalar volume element and the corresponding volume form of $\mathfrak{M}$ are[56]

$$\mathrm{d}V = \sqrt{G}\mathrm{d}X^1\mathrm{d}X^2\mathrm{d}X^3, \qquad d\Omega = \sqrt{G}\mathrm{d}X^1 \wedge \mathrm{d}X^2 \wedge \mathrm{d}X^3. \tag{15}$$

The area form corresponding to a compact region of $\mathfrak{M}$ is

$$\Omega = \sqrt{B}\mathrm{d}U^1 \wedge \mathrm{d}U^2. \tag{16}$$

The embedding of $\partial\mathfrak{M}$ in $\mathfrak{M}$ is represented by the local parametric equations $X^A = X^A(U^\alpha)\,(\alpha = 1, 2)$, $B^A_\alpha = \frac{\partial X^A}{\partial U^\alpha}$, and $B = \det(B^A_\alpha G_{AB} B^B_\beta)$. See references 57 and 58 for a comprehensive treatment of surfaces in (Riemannian) geometry. The following identities are also noted:

$$\delta_A(\ln\sqrt{G}) = \Gamma^B_{AB}, \qquad (\sqrt{G})_{|A} = \partial_A(\sqrt{G}) - N^B_A\bar{\partial}_B(\sqrt{G}) - \sqrt{G}H^B_{AB}. \tag{17}$$

Stokes' theorem in terms of a generic C^1 differentiable form $\boldsymbol{\alpha}$ is

$$\int_{\mathfrak{M}} d\boldsymbol{\alpha} = \oint_{\partial\mathfrak{M}} \boldsymbol{\alpha}. \tag{18}$$

Let $\boldsymbol{\alpha}(X, D) = V^A(X, D)\Omega(X, D)$ be a 2-form in Eq. 18, and let V^A be contravariant components of vector field $\boldsymbol{V} = V^A\frac{\delta}{\delta X^A}$. Let the horizontal connection be such that the second of Eq. 17 vanishes; for example, $H^B_{AB} = \Gamma^B_{AB} \to (\sqrt{G})_{|A} = 0$. Then in a coordinate chart $\{X^A\}$, Eq. 18 becomes[56]

$$\int_{\mathfrak{M}} [V^A_{|A} + (V^A C^C_{BC} + \bar{\partial}_B V^A)D^B_{;A}]d\Omega = \oint_{\partial\mathfrak{M}} V^A N_A \Omega, \tag{19}$$

where N_A is the unit outward normal to the domain of integration, $V^A_{|A} = \delta_A V^A + V^A H^B_{BA}$, and $D^B_{;A} = \partial_A D^B + N^B_A$.

2.2 Deformed Configuration Geometry

The current configuration is identified with a particular instant in time at which a solid body is considered deformed. The present discussion fully parallels that of Section 2.1 but with an adjustment in notation for deformed coordinates and their indices, which are denoted via lowercase rather than capital fonts. A differential manifold $\mathfrak{m}$ of spatial dimension 3 is identified with a deformed solid body embedded in ambient Euclidean 3-space. Let $x \in \mathfrak{m}$ denote a spatial point, and let $\{x^a\}(a = 1, 2, 3)$ denote a coordinate chart that is assumed to completely cover $\mathfrak{m}$, which may correspondingly be taken, by inessential assumption, for now as simply connected. Any assumption of simple connectivity will be relaxed later in the context of applications involving discontinuous motions associated with fracture, shear banding, and cavity formation; in such cases an atlas consisting of multiple charts may be needed to adequately cover the deformed body. Attached to each point is a vector $\boldsymbol{d}$, or equivalently, a chart of secondary coordinates $\{d^a\}(a = 1, 2, 3)$ is assigned that is treated as a field description of microstructure and can be associated with a second manifold $\mathfrak{u}$ of dimension 3. Herein, $\boldsymbol{d}$ need not be of unit length. One may now likewise assume $\mathfrak{u}$ is simply connected and covered by a single chart for simplicity, though the theory developed in this report may be readily applied toward bodies that are not simply connected.

Again following the notation of reference 14, the deformed state of the body can be couched in terms of pseudo-Finsler geometry. Define $\ddagger = (\mathfrak{z}, \pi, \mathfrak{m}, \mathfrak{u})$ as a fiber bundle of total (pseudo-Finsler) space $\mathfrak{z}$ (dimension 6), where $\pi : \mathfrak{z} \to \mathfrak{m}$ is the projection and $\mathfrak{u}$ the fiber. A chart covering $\mathfrak{z}$ is $\{x, d\}$. The natural/holonomic basis on $\mathfrak{z}$ is $\{\frac{\partial}{\partial x^a}, \frac{\partial}{\partial d^a}\}$. Coordinate transformations from $\{x, d\}$ to another chart $\{\tilde{x}, \tilde{d}\}$ are

$$\tilde{x}^a = \tilde{x}^a(x^1, x^2, x^3), \qquad \tilde{d^a}(x) = q^a_b(X)d^b. \tag{20}$$

Letting $q^a_b = \frac{\partial \tilde{x}^a}{\partial x^b}$, holonomic basis vectors on $T\mathfrak{z}$ transform as

$$\frac{\partial}{\partial \tilde{x}^a} = \frac{\partial x^b}{\partial \tilde{x}^a}\frac{\partial}{\partial x^b} + \frac{\partial^2 x^b}{\partial \tilde{x}^a \partial \tilde{x}^c}\tilde{d^c}\frac{\partial}{\partial d^b}, \qquad \frac{\partial}{\partial \tilde{d}^a} = \frac{\partial x^b}{\partial \tilde{x}^a}\frac{\partial}{\partial d^b}. \tag{21}$$

Let $n^a_b(x, d)$ denote nonlinear connection coefficients. Nonholonomic basis vectors are

$$\frac{\delta}{\delta x^a} = \frac{\partial}{\partial x^a} - n^b_a\frac{\partial}{\partial d^b}, \qquad \delta d^a = dd^a + n^a_b dx^b. \tag{22}$$

The set $\{\frac{\delta}{\delta x^a}, \frac{\partial}{\partial d^a}\}$ serves as a convenient local basis on $T\mathfrak{z}$, and $\{dx^a, \delta d^a\}$ for $T^*\mathfrak{z}$. The Sasaki metric tensor in spatial coordinates is

$$\boldsymbol{g}(x,d) = g_{ab}(x,d)dx^a \otimes dx^b + g_{ab}(x,d)\delta d^a \otimes \delta d^b. \tag{23}$$

Components g_{ab} and inverse components g^{ab} are used to lower and raise indices, and $g(x,d) = \det[g_{ab}(x,d)]$. Spatial differentiation is written in condensed form as

$$\partial_a(\cdot) = \frac{\partial(\cdot)}{\partial x^a}, \quad \bar{\partial}_a(\cdot) = \frac{\partial(\cdot)}{\partial d^a}; \qquad \delta_a(\cdot) = \frac{\delta(\cdot)}{\delta x^a} = \partial_a(\cdot) - n_a^b\bar{\partial}_b(\cdot). \tag{24}$$

Christoffel symbols of the second kind for the Levi-Civita connection on $\mathfrak{m}$ are

$$\gamma_{bc}^a = \tfrac{1}{2}g^{ad}(\partial_c g_{bd} + \partial_b g_{cd} - \partial_d g_{bc}) = g^{ad}\gamma_{bcd}. \tag{25}$$

Cartan's tensor in the current configuration is defined as

$$C_{bc}^a = \tfrac{1}{2}g^{ad}(\bar{\partial}_c g_{bd} + \bar{\partial}_b g_{cd} - \bar{\partial}_d g_{bc}) = g^{ad}C_{bcd}. \tag{26}$$

Horizontal coefficients of the spatial Chern-Rund and Cartan connections are

$$\Gamma_{bc}^a = \tfrac{1}{2}g^{ad}(\delta_c g_{bd} + \delta_b g_{cd} - \delta_d g_{bc}) = g^{ad}\Gamma_{bcd}. \tag{27}$$

Spatial components of the spray and derived nonlinear connection coefficents are, respectively,

$$g^a = \tfrac{1}{2}\gamma_{bc}^a d^b d^c, \qquad g_b^a = \bar{\partial}_b g^a. \tag{28}$$

Letting ∇ denote the covariant derivative, horizontal gradients of basis vectors are determined by the generic affine connection coefficients H_{bc}^a and K_{bc}^a:

$$\nabla_{\delta/\delta x^b}\frac{\delta}{\delta x^c} = H_{bc}^a\frac{\delta}{\delta x^a}, \qquad \nabla_{\delta/\delta x^b}\frac{\partial}{\partial d^c} = K_{bc}^a\frac{\partial}{\partial d^a}. \tag{29}$$

Vertical gradients are denoted by the generic connection coefficients V_{bc}^a and Y_{bc}^a:

$$\nabla_{\partial/\partial d^b}\frac{\partial}{\partial d^c} = V_{bc}^a\frac{\partial}{\partial d^a}, \qquad \nabla_{\partial/\partial d^b}\frac{\delta}{\delta x^c} = Y_{bc}^a\frac{\delta}{\delta x^a}. \tag{30}$$

The spatial configuration correlates with Finsler rather than pseudo-Finsler space when a C^∞ fundamental scalar function $\mathfrak{l}(x,d)$ exists at every point of $\mathfrak{u}\setminus 0$, homo-

geneous of degree one in $\boldsymbol{d}$, from which

$$g_{ab} = \tfrac{1}{2}\bar{\partial}_a\bar{\partial}_b(\mathfrak{l}^2), \qquad g^a_b = \gamma^a_{bc}d^c - C^a_{bc}\gamma^c_{de}d^d d^e = \Gamma^a_{bc}d^c, \qquad C_{abc} = \tfrac{1}{4}\bar{\partial}_a\bar{\partial}_b\bar{\partial}_c(\mathfrak{l}^2). \tag{31}$$

The Chern-Rund connection is invoked when Eq. 31 holds and $n^a_b = g^a_b, H^a_{bc} = K^a_{bc} = \Gamma^a_{bc}, V^a_{bc} = Y^a_{bc} = 0$; the Cartan connection is invoked when Eq. 31 holds and $n^a_b = g^a_b, H^a_{bc} = K^a_{bc} = \Gamma^a_{bc}, V^a_{bc} = Y^a_{bc} = C^a_{bc}$. Let $(\cdot)_{|c}$ denote horizontal covariant differentiation in a spatial chart $\{x^c\}$. Then when either of these connections is used, the horizontal covariant derivative of $\boldsymbol{g}$ vanishes:

$$g_{ab|c} = \delta_c g_{ab} - \Gamma^d_{ca}g_{db} - \Gamma^d_{cb}g_{da} = \partial_c g_{ab} - n^d_c\bar{\partial}_d g_{ab} - \Gamma^d_{ca}g_{db} - \Gamma^d_{cb}g_{da} = 0. \tag{32}$$

A (pseudo)-Finsler space degenerates to a Riemannian space when $g_{ab}(x,d) \to g_{ab}(x)$, and to a locally Minkowskian space when $\mathfrak{l}(x,d) \to \mathfrak{l}(d)$.

Let $\mathrm{d}\boldsymbol{x}$ denote a differential line element on $\mathfrak{m}$ and $\mathrm{d}\boldsymbol{d}$ denote a corresponding element on $\mathfrak{u}$. Squared lengths of these elements with respect to Eq. 23 are

$$|\mathrm{d}\boldsymbol{x}|^2 = \langle \mathrm{d}\boldsymbol{x}, \boldsymbol{g}\mathrm{d}\boldsymbol{x}\rangle = g_{ab}\mathrm{d}x^a\mathrm{d}x^b, \qquad |\mathrm{d}\boldsymbol{d}|^2 = \langle \mathrm{d}\boldsymbol{d}, \boldsymbol{g}\mathrm{d}\boldsymbol{d}\rangle = g_{ab}\mathrm{d}d^a\mathrm{d}d^b. \tag{33}$$

The scalar volume element and volume form of $\mathfrak{m}$ are

$$\mathrm{d}v = \sqrt{g}\mathrm{d}x^1\mathrm{d}x^2\mathrm{d}x^3, \qquad d\omega = \sqrt{g}\mathrm{d}x^1 \wedge \mathrm{d}x^2 \wedge \mathrm{d}x^3. \tag{34}$$

By a simple change of notation from referential to spatial quantities, an area form ω can be introduced analogously to Ω in Eq. 16, as can spatial versions of the coordinate-free Stokes' theorem in Eq. 18 and Rund's horizontal divergence theorem in Eq. 19.

2.3 Deformation Kinematics

Transformations from referential to spatial coordinates ($\mathfrak{M}$ to $\mathfrak{m}$) and vice versa are denoted by the C^2 functions

$$x^a(X,D) = \varphi^a[X, D(X)], \qquad X^A(x,d) = \Phi^A[x, d(x)]. \tag{35}$$

Since the present theory is quasi-static, time does not enter such functions as an explicit independent variable. Incorporation of the internal state (D or d) in these

motion functions distinguishes Finsler kinematics[14,33] from the usual kinematics in Riemannian geometry of classical continuum physics.[25,59] State vector mappings are of the affine form

$$d^a(X,D) = \vartheta^a[X, D(X)] = \vartheta^a_B(X) D^B, \quad D^A(x,d) = \Theta^A[x, d(x)] = \Theta^A_b(x) d^b. \tag{36}$$

The deformation gradient from reference to current (pseudo)-Finsler tangent spaces is defined as the delta derivative

$$\begin{aligned} \boldsymbol{F}(X,D) &= F^a_A(X,D) \frac{\delta}{\delta x^a} \otimes dX^A = \frac{\delta \varphi^a(X,D)}{\delta X^A} \frac{\delta}{\delta x^a} \otimes dX^A = \frac{\delta \boldsymbol{x}(X,D)}{\delta \boldsymbol{X}}, \\ F^a_A &= \delta_A \varphi^a = \partial_A x^a - N^B_A \bar{\partial}_B x^a. \end{aligned} \tag{37}$$

The analogous mapping from spatial to referential tangent spaces is the 2-point tensor

$$\begin{aligned} \boldsymbol{f}(x,d) &= f^A_a(x,d) \frac{\delta}{\delta X^A} \otimes dx^a = \frac{\delta \Phi^A(x,d)}{\delta x^a} \frac{\delta}{\delta X^A} \otimes dx^a = \frac{\delta \boldsymbol{X}(x,d)}{\delta \boldsymbol{x}}, \\ f^A_a &= \delta_a \Phi^A = \partial_a X^A - n^b_a \bar{\partial}_b X^A. \end{aligned} \tag{38}$$

Herein, for a 2-point tensor such as $\boldsymbol{F}$ in Eq. 37 and using Eq. 35, define

$$\partial_A x^a[X, D(X)] = \frac{\partial x^a(X,D)}{\partial X^A} + \frac{\partial x^a(X,D)}{\partial D^B} \frac{\partial D^B(X)}{\partial X^A}, \tag{39}$$

with an analogous definition of $\partial_a X^A[x, d(x)]$ in Eq. 38:

$$\partial_a X^A[x, d(x)] = \frac{\partial X^A(x,d)}{\partial x^a} + \frac{\partial X^A(x,d)}{\partial d^b} \frac{\partial d^b(x)}{\partial x^a}. \tag{40}$$

Transformation equations for differential line elements follow by generalizing fundamental postulates of continuum mechanics in Riemannian space[25,59] to account for the nonholonomic bases of Finsler space, whereby partial coordinate derivatives are replaced with delta-derivatives:

$$\mathrm{d}\boldsymbol{x} = \frac{\delta \boldsymbol{x}}{\delta \boldsymbol{X}} \mathrm{d}\boldsymbol{X} \Leftrightarrow \mathrm{d}x^a = F^a_A \mathrm{d}X^A, \qquad \mathrm{d}\boldsymbol{X} = \frac{\delta \boldsymbol{X}}{\delta \boldsymbol{x}} \mathrm{d}\boldsymbol{x} \Leftrightarrow \mathrm{d}X^A = f^A_a \mathrm{d}x^a. \tag{41}$$

It follows that volume elements and volume forms transform between reference and

spatial frames as

$$\begin{aligned} \mathrm{d}v = J\mathrm{d}V = [\det(F_A^a)\sqrt{g/G}]\mathrm{d}V, \qquad d\omega = Jd\Omega; \\ \mathrm{d}V = j\mathrm{d}v = [\det(f_a^A)\sqrt{G/g}]\mathrm{d}v, \qquad d\Omega = jd\omega. \end{aligned} \tag{42}$$

Lengths of deformed and initial line elements can be compared using the deformation tensor $\boldsymbol{C}$:

$$|\mathrm{d}\boldsymbol{x}|^2 = F_A^a F_B^b g_{ab} \mathrm{d}X^A \mathrm{d}X^B = C_{AB}\mathrm{d}X^A\mathrm{d}X^B = \langle \mathrm{d}\boldsymbol{X}, \boldsymbol{C}\mathrm{d}\boldsymbol{X}\rangle, \tag{43}$$

where

$$\boldsymbol{C} = C_{AB} dX^A \otimes dX^B = F_A^a g_{ab} F_B^b dX^A \otimes dX^B. \tag{44}$$

It follows that $\det(C_{AB}) = J^2 G$. For the directors or state vectors, a similar construction using Eq. 36 gives

$$|\boldsymbol{d}|^2 = \vartheta^a \vartheta_a = \Xi_{AB} D^A D^B = \langle \boldsymbol{D}, \boldsymbol{\Xi D}\rangle, \tag{45}$$

with

$$\boldsymbol{\Xi} = \Xi_{AB} \delta D^A \otimes \delta D^B = \vartheta_A^a g_{ab} \vartheta_B^b \delta D^A \otimes \delta D^B. \tag{46}$$

A transformation rule for gradients of nonholonomic bases is obtained from definitions Eq. 29 and Eq. 37:

$$\nabla_{\delta/\delta X^A} \frac{\delta}{\delta x^c} = \frac{\delta x^a}{\delta X^A} \nabla_{\delta/\delta x^a} \frac{\delta}{\delta x^c} = F_A^a \nabla_{\delta/\delta x^a} \frac{\delta}{\delta x^c} = F_A^a H_{ac}^b \frac{\delta}{\delta x^b}. \tag{47}$$

This transformation, which is used later in the total covariant derivative operation[25] extended here to 2-point tensors in Finsler space, provides further motivation for the presently proposed definition of the deformation gradient $\boldsymbol{F}$ as a delta-derivative.

3. Energy Functional and Conservation Laws

The following variational principle is set forth, where Ψ is the action integral for a closed and simply connected region of $\mathfrak{M}$ with boundary $\partial\mathfrak{M}$, and surface forces are $\boldsymbol{p} = p_a dx^a$, a mechanical load vector (force per unit reference area), and $\boldsymbol{z} = z_A \delta D^A$, a thermodynamic force conjugate to the internal state vector:

$$\delta\Psi(\boldsymbol{\varphi}, \boldsymbol{D}) = \oint_{\partial\mathfrak{M}} (\langle \boldsymbol{p}, \delta\boldsymbol{x}\rangle + \langle \boldsymbol{z}, \delta\boldsymbol{D}\rangle)\Omega. \tag{48}$$

Letting ψ denote potential energy density (i.e., internal or free energy density in the absence of kinetic and thermal effects), this becomes

$$\delta \int_{\mathfrak{M}} \psi d\Omega = \oint_{\partial\mathfrak{M}} [p_a \delta x^a + z_A \delta(D^A)]\Omega, \tag{49}$$

where the first variation of $\boldsymbol{D}$ is enclosed in parentheses to avoid confusion with basis vector δD^A. The following functional form of the energy density per unit reference volume on $\mathfrak{M}$ is assumed:

$$\psi = \psi(\boldsymbol{F}, \boldsymbol{D}, \nabla\boldsymbol{D}, \boldsymbol{G}) = \psi(F^a_A, D^A, D^A_{|B}, G_{AB}). \tag{50}$$

This form of the energy density is motivated by phase field theory,[43,60] whereby the internal state vector $\boldsymbol{D}$ is treated here analogously to an order parameter. Further motivation is obtained from continuum mechanical models of liquid crystals, wherein director vector gradients may enter the thermodynamic potentials.[61] Later in Sections 4, 5, and 6, a more precise physical meaning will be assigned to the internal state vector in the context of example problems. Thermodynamic forces are introduced by taking the first variation of Eq. 50:

$$\begin{aligned} \delta\psi &= \frac{\partial\psi}{\partial F^a_A}\delta F^a_A + \frac{\partial\psi}{\partial D^A}\delta(D^A) + \frac{\partial\psi}{\partial D^A_{|B}}\delta D^A_{|B} + \frac{\partial\psi}{\partial G_{AB}}\delta G_{AB} \\ &= P^A_a \delta F^a_A + Q_A \delta(D^A) + Z^B_A \delta D^A_{|B} + S^{AB}\delta G_{AB}. \end{aligned} \tag{51}$$

Imposition of spatial coordinate invariance leads to the restricted form

$$\psi = \psi[\boldsymbol{C}(\boldsymbol{F}, \boldsymbol{g}), \boldsymbol{D}, \nabla\boldsymbol{D}, \boldsymbol{G}] = \psi(C_{AB}, D^A, D^A_{|B}, G_{AB}), \tag{52}$$

from which the first Piola-Kirchhoff stress P^A_a and Cauchy stress σ^{ab} obey

$$P^A_a = 2g_{ab}F^b_B \frac{\partial\psi}{\partial C_{AB}}, \qquad \sigma^{ab} = jg^{ac}P^A_c F^b_A = 2jF^a_A F^b_B \frac{\partial\psi}{\partial C_{AB}} = \sigma^{ba}. \tag{53}$$

Symmetry of Cauchy stress is consistent with the balance of angular momentum of classical continuum mechanics.[19,59]

Noting that variation $\delta(\cdot)$ is performed with X fixed but D variable,

$$\delta F^a_A = \delta_A(\delta\varphi^a) - \bar{\partial}_B\varphi^a \bar{\partial}_C N^B_A \delta(D^C), \tag{54}$$

$$\delta D^A_{|B} = [\delta(D^A)]_{|B} - (\bar{\partial}_C N^A_B - \bar{\partial}_C K^A_{BD} D^D)\delta(D^C), \tag{55}$$

$$\delta(d\Omega) = G^{AB}\bar{\partial}_C G_{AB}\delta(D^C)d\Omega. \tag{56}$$

Substituting Eq. 51 and Eq. 54–Eq. 56 into the left side of Eq. 49 gives

$$\begin{aligned}\delta\int_{\mathfrak{M}}\psi d\Omega = \int_{\mathfrak{M}}\{&P^A_a\delta_A(\delta\varphi^a) + Z^B_A[\delta(D^A)]_{|B} \\ &+ [Q_C - P^A_a\bar{\partial}_B\varphi^a\bar{\partial}_C N^B_A - Z^B_A(\bar{\partial}_C N^A_B - \bar{\partial}_C K^A_{BD}D^D) \\ &+ (S^{AB} + \psi G^{AB})\bar{\partial}_C G_{AB}]\delta(D^C)\}d\Omega.\end{aligned} \tag{57}$$

Two applications of the divergence theorem Eq. 19 and repeated integration by parts then gives the following equivalent integral form of Eq. 49:

$$\begin{aligned}-\int_{\mathfrak{M}}\{&[P^A_{a|A} + (P^A_a C^C_{BC} + \bar{\partial}_B P^A_a)D^B_{;A}]\delta\varphi^a + [Q_C - Z^B_{C|B} \\ &- (Z^A_C C^D_{BD} + \bar{\partial}_B Z^A_C)D^B_{;A} - Z^B_A(\bar{\partial}_C N^A_B - \bar{\partial}_C K^A_{BD}D^D) \\ &- P^A_a(\bar{\partial}_B\bar{\partial}_C\varphi^a D^B_{;A} + \bar{\partial}_B\varphi^a\bar{\partial}_C N^B_A) + (S^{AB} + \psi G^{AB})\bar{\partial}_C G_{AB}]\delta(D^C)\}d\Omega \\ &+ \oint_{\partial\mathfrak{M}}[P^A_a N_A\delta\varphi^a + Z^B_A N_B\delta(D^A)]\Omega = \oint_{\partial\mathfrak{M}}[p_a\delta\varphi^a + z_A\delta(D^A)]\Omega.\end{aligned} \tag{58}$$

Assuming this global equation must hold for admissible variations $\delta\boldsymbol{x}$ and $\delta\boldsymbol{D}$, local results from Eq. 58 are the Euler-Lagrange equations (i.e., force balances) and the Neumann boundary conditions:

$$\partial_A P^A_a + P^B_a H^A_{AB} - P^A_c H^c_{ba} F^b_A + P^A_a N^B_A C^C_{BC} + (P^A_a C^C_{BC} + \bar{\partial}_B P^A_a)\partial_A D^B = 0, \tag{59}$$

$$\begin{aligned}\partial_A Z^A_C &+ Z^B_C H^A_{AB} - Z^A_B H^B_{AC} + \bar{\partial}_B Z^A_C\partial_A D^B \\ &+ Z^B_A(\bar{\partial}_C N^A_B - \bar{\partial}_C K^A_{BD}D^D + \delta^A_C C^D_{ED}D^E_{;B}) \\ &+ P^A_a(\bar{\partial}_B\bar{\partial}_C\varphi^a D^B_{;A} + \bar{\partial}_B\varphi^a\bar{\partial}_C N^B_A) - (S^{AB} + \psi G^{AB})\bar{\partial}_C G_{AB} = Q_C;\end{aligned} \tag{60}$$

$$p_a = P^A_a N_A, \qquad z_A = Z^B_A N_B. \tag{61}$$

Note that Eq. 47 has been used in Eq. 59 for determining the (total) horizontal covariant derivative of the 2-point tensor $\boldsymbol{P} = P^A_a dx^a \otimes \frac{\delta}{\delta X^A}$. Equation 59 is the (local) balance of linear momentum for quasi-statics. Equation 60 will be referred to as the (local) balance of director momentum or micromomentum.

Balance Eqs. 59 and 60 reduce as follows when configuration spaces are (pseudo)-

Riemannian (***G*** independent of D):

$$\partial_A P_a^A + P_a^B \gamma_{AB}^A - P_c^A \gamma_{ba}^c \partial_A \varphi^b + \bar{\partial}_B P_a^A \partial_A D^B = 0, \tag{62}$$

$$\partial_A Z_C^A + Z_C^B \gamma_{AB}^A - Z_B^A \gamma_{AC}^B + \bar{\partial}_B Z_C^A \partial_A D^B + P_a^A \bar{\partial}_B \bar{\partial}_C \varphi^a \partial_A D^B = Q_C; \tag{63}$$

(pseudo)-Minkowskian (***G*** independent of X and ***g*** independent of x):

$$\partial_A P_a^A + (P_a^A C_{BC}^C + \bar{\partial}_B P_a^A) \partial_A D^B = 0, \tag{64}$$

$$\begin{aligned} \partial_A Z_C^A + \bar{\partial}_B Z_C^A \partial_A D^B + Z_C^B C_{AD}^D \partial_B D^A + P_a^A \bar{\partial}_B \bar{\partial}_C \varphi^a \partial_A D^B \\ - (S^{AB} + \psi G^{AB}) \bar{\partial}_C G_{AB} = Q_C; \end{aligned} \tag{65}$$

and Cartesian (global metrics $G_{AB} = \delta_{AB}$ and $g_{ab} = \delta_{ab}$):

$$\partial_A P_a^A + \bar{\partial}_B P_a^A \partial_A D^B = 0, \tag{66}$$

$$\partial_A Z_C^A + \bar{\partial}_B Z_C^A \partial_A D^B + P_a^A \bar{\partial}_B \bar{\partial}_C \varphi^a \partial_A D^B = Q_C. \tag{67}$$

The model framework is complete upon prescription of the following details. For pseudo-Finsler reference space, a metric tensor ***G*** is introduced over the domain of interest in $\mathfrak{Z}$, from which all connection coefficients are derived via differentiation using relations listed in Section 2.1. In this regard, nonlinear coefficients can be determined from the spray in Eq. 9, and particular forms for horizontal and vertical connection coefficients in Eqs. 10 and 11 must be prescribed (i.e., those corresponding the Chern-Rund connection or Cartan's connection). The main requirement for selection of horizontal coefficients is that $(\sqrt{G})_{|A}$ must vanish for the form of divergence theorem in Eq. 19 to apply; this is true for Chern-Rund and Cartan connections. Anaolgous choices must be prescribed for the current configuration space, including specification of metric tensor ***g***, from which connection coefficients are derived via equations in Section 2.2. Note that the same forms of metric and connections need not be prescribed in both configurations; that is, the reference space could be taken as Finslerian and the current configuration space Riemannian, or vice-versa. Regarding deformation kinematics of Section 2.3, a constitutive equation may be added for specification of transformation matrix ϑ_B^a in Eq. 36, but this is not essential for the solution of all boundary value problems. For crystals, a convenient assumption is the Cauchy-Born rule,[62,63] whereby $\vartheta_A^a(X) = F_A^a[X, D(X)]$

in a consistent coordinate basis. A particular form of free energy function ψ in Eq. 50 physically appropriate for the material of interest must also be invoked. Then, given prescribed boundary conditions on $\partial\mathfrak{M}$, governing Eqs. 59 and 60 represent, in principle, 6 coupled nonlinear partial differential equations for 6 unknown fields $\varphi^a[X, D(X)]$ and $D^A(X)$. If Finsler geometry rather than pseudo-Finsler geometry is presumed, then a fundamental scalar function $\mathfrak{L}$ is introduced that provides $\boldsymbol{G}$ by differentiation via Eq. 12 rather than direct prescription, and similarly for $\mathfrak{l}$ and $\boldsymbol{g}$ via Eq. 31.

A few major differences from prior literature are noted. Specifically, the new definition used herein for the deformation gradient (2-point) tensor in Eq. 37—a delta-derivative—differs from that in reference 12—a partial derivative—and that in references 33 and 41—a covariant derivative—and can be interpreted as a compromise between the other latter; this compromise further enables computation of Eq. 47. Certain choices or options for metric tensors and connection coefficients also vary among the present work and these prior works, and the form of free energy function in Eq. 50 differs from that proposed in references 33 and 41.

4. Physics of Fracture

The first of 3 boundary value problems is considered in the present section. By construction, these problems involve fields that could vary in only 1 or 2 rather than all 3 spatial directions. Two strategies are possible for formulating the pseudo-Finsler theory to solve such problems: either define a general 3-D theory and then reduce the equations appropriately for the problem geometry, or construct a theory of reduced dimensionality from the outset. The latter approach is taken in Section 4 to obtain physical insight while maintaining mathematical simplicity.

4.1 Problem Geometry and Kinematics

Considered first is perhaps the simplest physically meaningful application of the theory. The material body is a straight 1-D bar of length L_0, and the material manifold is specified as $\{\mathfrak{M} : X \in [0, L_0]\}$. By construction, fields vary only with $X = X^1$ and $D = D^1$, and coordinates X^2, X^3, D^2, D^3 are superfluous. A Cartesian coordinate system suffices for $\{X\}$, so there is no need to assign a metric tensor with dependence on X. Consistent with these protocols, the following relations, which are reductions of more general definitions and identities of Section 2.1,

apply:

$$X = X^1, \quad D = D^1; \qquad G = G_{11}(D), \quad G^{11}(D) = 1/G(D); \tag{68}$$

$$\gamma_{111} = \tfrac{1}{2}\partial_1 G = 0, \quad \gamma^1_{11} = 0; \quad G^1 = \tfrac{1}{2}\gamma^1_{11} D^1 D^1 = 0, \quad N^1_1 = \bar{\partial}_1 G^1 = 0; \tag{69}$$

$$C_{111} = \tfrac{1}{2}\bar{\partial}_1 G = G'/2, \qquad C^1_{11} = G'/(2G). \tag{70}$$

The reference configuration space is locally Minkowskian. Invoking the Chern-Rund connection with vanishing nonlinear connection coefficients from Eq. 69,

$$H^1_{11} = K^1_{11} = \Gamma^1_{11} = \tfrac{1}{2G}\delta_1 G = 0; \qquad V^1_{11} = Y^1_{11} = 0. \tag{71}$$

For the current/deformed configuration of the bar, with deformed material manifold $\{\mathfrak{m} : x \in [0, L]\}$, with L the deformed length of the domain, spatial coordinates and metric components are of the assumed Cartesian form

$$x = x^1, \quad d = d^1; \qquad g = g_{11} = 1, \quad g^{11} = 1/g = 1. \tag{72}$$

All spatial connection coefficients of Section 2.2—linear and nonlinear—then vanish identically.

Motions, deformations, and director gradients defined in Section 2.3 reduce as follows for the current 1-D problem:

$$x = \varphi(X, D), \qquad d = \vartheta(X, D); \qquad D = D(X); \tag{73}$$

$$F(X, D) = F^1_1(X, D) = \delta_1 x^1(X, D) = \frac{\partial \varphi(X, D)}{\partial X} + \frac{\partial \varphi(X, D)}{\partial D}\frac{\partial D(X)}{\partial X}; \tag{74}$$

$$J(X, D) = \sqrt{g/G(D)} F^1_1(X, D) = [G(D)]^{-1/2}[F(X, D)]; \tag{75}$$

$$C(X, D) = C_{11}(X, D) = F^1_1(X, D) g_{11} F^1_1(X, D) = [F(X, D)]^2; \tag{76}$$

$$D^1_{|1} = \partial_1 D - N^1_1 + K^1_{11} D = \partial D/\partial X = D'. \tag{77}$$

The internal state variable D is physically identified with crack opening displacement. Define a total strain measure ϵ (which includes a microdeformation gradient contribution) and a lattice strain measure a associated with stored elastic energy as,

respectively,

$$\epsilon = \sqrt{C} - 1 = F - 1; \qquad a = \epsilon - D' = \epsilon - \frac{\partial D}{\partial X} = \frac{\partial}{\partial X}(x - X - D). \quad (78)$$

Stretch occurs for $\epsilon > 0$, contraction for $\epsilon < 0$. Also introduce a constant l with dimensions of length and a normalized order parameter ξ:

$$\xi = D/l, \qquad \xi' = D'/l; \qquad a = \epsilon - l\xi'. \quad (79)$$

Constant l will later be identified as the value of crack opening displacement at which the bar supports no tensile load. Letting k denote a constant depending on the material of interest, a more specific form of the Minkowski metric in Eq. 68 is introduced as

$$G(\xi) = \exp(2k\xi) \Rightarrow G'/(2G) = C^1_{11} = k/l. \quad (80)$$

The length of a referential line element in Eq. 14 and the corresponding volume form in Eq. 15 become

$$|\mathrm{d}X|^2 = \mathrm{d}X \cdot G \cdot \mathrm{d}X = \exp(2kD/l)\mathrm{d}X \cdot \mathrm{d}X, \quad d\Omega = \sqrt{G}\mathrm{d}X = \exp(kD/l)\mathrm{d}X, \quad (81)$$

such that expansion occurs when $k > 0$ and contraction when $k < 0$ if $\xi > 0$. The former case is physically representative of microscopic dilatation from cracking in crystalline rocks, for example[44,46] as well as dilatation from core fields of dislocations[18,39,47] that may emerge in the vicinity of crack tips in more ductile crystals. Volume changes due to thermal expansion or contraction might also be represented via such a description. Because G is not homogeneous of degree zero in D, the reference configuration space is not strictly of Finsler character, but rather is labeled a pseudo-Finsler space.[16] Furthermore, because G does not depend explicitly on X, this space may be categorized as pseudo-Minkowskian.

4.2 Energy, Thermodynamic Forces, and Balance Laws

Application of results derived in Section 4.1 leads to the following forms of Eqs. 50 and 52 for the present 1-D example:

$$\psi = \psi(C, D, \partial D/\partial X, G) = \psi(F, D, \partial D/\partial X, G) = \psi(\epsilon, D, \partial D/\partial X, G). \quad (82)$$

Written in terms of lattice strain and normalized order parameter, this becomes

$$\psi = \psi[a(\epsilon, \xi'), \xi, \xi', G(\xi)]. \tag{83}$$

Motivated again by phase field theory,[43,60] the following sum of quadratic forms is invoked:

$$\psi = \tfrac{1}{2}\Lambda(1-\xi)^2 a^2 + \Upsilon\xi^2/l + \Upsilon l(\xi')^2. \tag{84}$$

Material constants are defined as follows: $\Lambda = \lambda + 2\mu$ is the longitudinal elastic stiffness, Υ is the crack surface energy per unit reference area, and regularization length l has been introduced already in Eq. 79. The first term on the right side of Eq. 84 accounts for elastic strain energy degraded by damage associated with $\xi \in [0, 1]$, and the other 2 terms combine to account for the surface energy of fracture. This energy function contains no explicit dependence on G.

Nonzero thermodynamic forces of Section 3 are then obtained by direct calculation as

$$P = P_1^1 = \frac{\partial\psi}{\partial\epsilon} = \frac{\partial\psi}{\partial a}\frac{\partial a(\epsilon,\xi')}{\partial\epsilon} = \Lambda(1-\xi)^2 a; \tag{85}$$

$$Q = Q_1 = \frac{\partial\psi}{\partial D} = \frac{1}{l}\frac{\partial\psi}{\partial\xi} = -\frac{\Lambda}{l}(1-\xi)a^2 + 2\frac{\Upsilon}{l^2}\xi = -\frac{Pa}{l(1-\xi)} + 2\frac{\Upsilon}{l^2}\xi; \tag{86}$$

$$Z = Z_1^1 = \frac{\partial\psi}{\partial D'} = \frac{1}{l}\frac{\partial\psi}{\partial\xi'} = 2\Upsilon\xi' + \frac{1}{l}\frac{\partial\psi}{\partial a}\frac{\partial a}{\partial\xi'} = 2\Upsilon\xi' - \Lambda(1-\xi)^2 a = 2\Upsilon\xi' - P. \tag{87}$$

The linear momentum balance in Eqs. 59 and 64 becomes

$$\frac{\partial P(X,D)}{\partial X} + \frac{\partial P(X,D)}{\partial D}\frac{\partial D}{\partial X} + P\frac{G'(D)}{2G(D)}\frac{\partial D}{\partial X} = \frac{\mathrm{d}P}{\mathrm{d}X} + P\frac{G'}{2G}\frac{\mathrm{d}D}{\mathrm{d}X} = 0. \tag{88}$$

The micromomentum balance in Eqs. 60 and 65 becomes

$$\begin{aligned}\frac{\partial Z(X,D)}{\partial X} + \left[\frac{\partial Z(X,D)}{\partial D} + Z\frac{G'(D)}{2G(D)} + P\frac{\partial^2\varphi(X,D)}{\partial D^2}\right]\frac{\partial D}{\partial X} \\ - \frac{G'(D)}{G(D)}\psi(X,D) = Q(X,D).\end{aligned} \tag{89}$$

Substituting from Eqs. 80 and 85–87, these balance laws become

$$\frac{\mathrm{d}P}{\mathrm{d}X} = -kP\frac{\mathrm{d}\xi}{\mathrm{d}X}; \qquad P\left[\frac{a}{1-\xi} + \frac{\partial^2\varphi}{\partial\xi^2}\xi'\right] + 2\Upsilon l\xi'' - 2\frac{\Upsilon}{l}\xi = 2k[\psi - \Upsilon l(\xi')^2]. \tag{90}$$

Relations in Eq. 90 constitute a pair of coupled nonlinear ordinary differential equations wherein field variables P, a, ξ, φ, and ψ depend ultimately on the independent variable X.

4.3 Problem Solutions: Riemannian Geometry

Considered first is the simple case wherein the referential configuration space is Riemannian (in fact, a Cartesian structure), with $k = 0 \rightarrow G = 1 =$ constant. Even though the space is Cartesian, the kinematics are still of Finsler character since φ can potentially depend on both D and X rather than just X as in classical continuum physics. Balance laws in Eq. 90 degenerate to

$$\frac{\mathrm{d}P}{\mathrm{d}X} = 0; \qquad P\left[\frac{a}{1-\xi} + \frac{\partial^2\varphi}{\partial\xi^2}\xi'\right] + 2\Upsilon l\xi'' - 2\frac{\Upsilon}{l}\xi = 0. \tag{91}$$

The first of Eq. 91 results immediately in constant stress over the length of the bar:

$$P = P_0 = \Lambda(1-\xi)^2 a = \text{constant}. \tag{92}$$

The solution of the second requires further specification of boundary conditions. Two particular problems corresponding to 2 different sets of boundary conditions are addressed next: homogeneous damage of the deformed bar over $[0, L]$ (i.e., microscopic fractures evenly distributed along the length of the bar) and localized damage corresponding to a globally stress-free deformed state (i.e., complete tensile fracture/rupture of the bar).

4.3.1 Homogeneous Damage

For homogeneous damage, $\xi'(X) = 0 \forall X \in [0, L_0] \Rightarrow \xi(0) = \xi(L_0) = \xi_H$. Boundary conditions on displacement are prescribed as follows:

$$\varphi(0, D) = \varphi_0 = D = l\xi_H, \quad \varphi(L_0, D) = \varphi_L = (1 + a_H)L_0 + l\xi_H. \tag{93}$$

Here, φ_L is the prescribed coordinate of the deformed bar at $x = L$, with a_H and ξ_H constants. Equations 91 and 92 result in

$$P_0 = \Lambda(1-\xi_H)^2 a_H, \qquad \xi_H = 1/[1 + 2\Upsilon/(\Lambda l a_H^2)]. \tag{94}$$

Given φ_L, the second of Eq. 93 and Eq. 94 can be solved simultaneously for the homogeneous damage field ξ_H, stress P_0, and stretch a_H. The problem kinematics

are consistent with the separable decomposition of the motion φ into

$$\varphi[X, \xi(D)] = \chi(X) + l\xi(D), \qquad F = \partial\varphi/\partial X = \chi', \tag{95}$$

where for homogeneous damage and strain fields,

$$\varphi[X, \xi_H] = (1 + a_H)X + l\xi_H, \qquad \chi = (1 + a_H)X, \qquad F = 1 + a_H. \tag{96}$$

The total energy of the degraded elastic bar is obtained as

$$\begin{aligned} \Psi(\varphi_L, \xi_H) = \Psi_H &= \int_0^{L_0} [\Lambda(1 - \xi_H)^2 a_H^2/2 + \Upsilon\xi_H^2/l]\mathrm{d}X \\ &= [\Lambda(1 - \xi_H)^2 a_H^2/2 + \Upsilon\xi_H^2/l]L_0. \end{aligned} \tag{97}$$

Remark: Letting $\varphi(X, D) \rightarrow \varphi(X) = \chi(X)$ and modifying Eq. 93 to $\varphi_0 = 0, \varphi_L = (1 + a_H)L_0$ recovers a description analogous to that of phase field theories of fracture mechanics.[43,64]

4.3.2 Stress-Free State

For a stress-free state, $P = P_0 = 0 \forall X \in [0, L_0]$. Boundary conditions on the order parameter $\xi(X)$ or internal state variable representing microdisplacement are prescribed as follows:

$$\xi(0) = D(0)/l = 1, \qquad \xi(L_0) = 0. \tag{98}$$

The second of the governing equations in Eq. 91 becomes the homogeneous linear second-order ordinary differential equation and corresponding exact solution

$$\xi'' - \xi/l^2 = 0 \Rightarrow \xi(X) = \frac{\exp(-X/l)}{1 - \exp(2L_0/l)}[\exp(2X/l) - \exp(2L_0/l)]. \tag{99}$$

The null stress condition results in $a(X) = 0 \forall \xi(X) \neq 1$; since lattice stretch $a(X)$ and $\varphi_0 = \varphi(0, D)$ are indeterminate where $\xi = 1$, the total displacement at the undamaged end of the bar, φ_L, is also indeterminate. Physically, this corresponds to rigidly displacing the bar, once disconnected from its fully fractured site at $X = 0$, without altering its internal energy. Total energy is the integral

$$\Psi(\xi) = \Psi_F = \int_0^{L_0} \Upsilon[(\xi')^2 l + \xi^2/l]\mathrm{d}X. \tag{100}$$

Remark: Equation 99 contains an equation and associated solution identical to that attainable through phase field theories of fracture mechanics.[43,64]

4.4 Problem Solutions: Minkowskian Geometry

Considered now is the more general case wherein the referential configuration space is pseudo-Finslerian (specifically, a locally Minkowskian structure) with $k \neq 0$ in Eq. 80. Even though the referential metric is pseudo-Minkowskian, deformation kinematics are again of Finsler nature since $x = \varphi(X, D)$ can potentially depend on D as well as X. Balance laws in Eq. 90 apply; the first results in

$$\mathrm{d}P/P = -k\mathrm{d}\xi \Rightarrow P = P_0 \exp(-k\xi), \tag{101}$$

where P_0 is the constant stress corresponding to $k = 0$ and/or $\xi = 0$. The solution of the second balance law again requires further specification of boundary conditions. The same 2 problems considered in Sections 4.3.1 and 4.3.2 are now revisited in the context of the pseudo-Minkowski metric in Eq. 80, recalling that $k > 0$ accounts for additional microscopic stretch and dilatation in the damaged zone neglected in the Riemannian metrical representation of Section 4.3.

4.4.1 Homogeneous Damage

For homogeneous damage, $\xi'(X) = 0 \forall X \in [0, L_0] \Rightarrow \xi(0) = \xi(L_0) = \xi_H$. Boundary conditions on displacement are identical to Eq. 93:

$$\varphi(0, D) = \varphi_0 = D = l\xi_H, \quad \varphi(L_0, D) = \varphi_L = (1 + a_H)L_0 + l\xi_H. \tag{102}$$

Equations 90 and 101 result in

$$\begin{aligned} P = P_H = P_0 \exp(-k\xi_H) = \Lambda(1 - \xi_H)^2 a_H = \text{constant}, \\ \Lambda a_H^2 (1 - \xi_H) - 2(\Upsilon/l)\xi_H = 2k\psi(a_H, \xi_H). \end{aligned} \tag{103}$$

Given φ_L, Eqs. 102 and 103 can be solved simultaneously for the homogeneous damage field ξ_H, stress P_0, and stretch a_H. The problem kinematics are consistent with the separable decomposition of Eqs. 95 and 96. The total energy of the elastic

bar is obtained as

$$\begin{aligned}\Psi(\varphi_L, \xi_H) = \Psi_H &= \int_0^{L_0} [\Lambda(1-\xi_H)^2 a_H^2/2 + \Upsilon \xi_H^2/l] \mathrm{d}X \\ &= [\Lambda(1-\xi_H)^2 a_H^2/2 + \Upsilon \xi_H^2/l] L_0,\end{aligned} \tag{104}$$

identical in form to Eq. 97 but with potentially different values of ξ_H and a_H for a prescribed φ_L when k is nonzero.

Shown in Fig. 1 are $\xi = \xi_H$, $P = P_H$, and $\Psi = \Psi_H$ versus applied tensile displacement, computed via Eqs. 103 and 104. Representative material parameters are taken as $\lambda = \mu = \Lambda/3 = 10^{11}\mathrm{N/m}^2$, $\Upsilon = 1\mathrm{N/m}$, and $l = 10^{-9}\mathrm{m}$.[43,60] The domain size is $L_0 = 10^3 l$, and the Weyl scaling parameter k is varied from 0 to $\ln 2$, with the latter (maximum considered) value corresponding to a maximum volume form scaling of $\sqrt{G} = 2$ at $\xi_H = 1$. Since resulting volume changes are considerably large, the Weyl scaling could be interpreted as giving rise to a fictitious damaged configuration, similar to that envisioned in nonlinear continuum damage mechanics.[65] For any fixed value of k, the order parameter ξ increases monotonically with increasing tensile displacement (Fig. 1a), tensile stress P increases to a maximum and then decreases (Fig. 1b), and energy Ψ increases monotonically (Fig. 1c). As k increases, the value of ξ tends to decrease for $0 < (\varphi_L/L_0 - 1) < 0.5$, while P and Ψ tend to increase over the same range of displacement. Notably, as evident from Fig. 1b, the peak stress and the applied displacement at which the peak stress is reached both increase significantly with increasing k, implying an increase in tensile strength and stability of the material commensurate with microscopic dilatation represented by positive values of k. The increases in stress and energy correlate with a decrease in order parameter since both P and strain energy density contain a multiplication factor of $(1-\xi)^2$. The contribution of the $l\xi_H$ term in Eq. 96 is negligible since $l/L_0 \ll 1$; therefore, differences between the present Finsler solution with $k = 0$ and phase field theory[43,64] are also negligible.

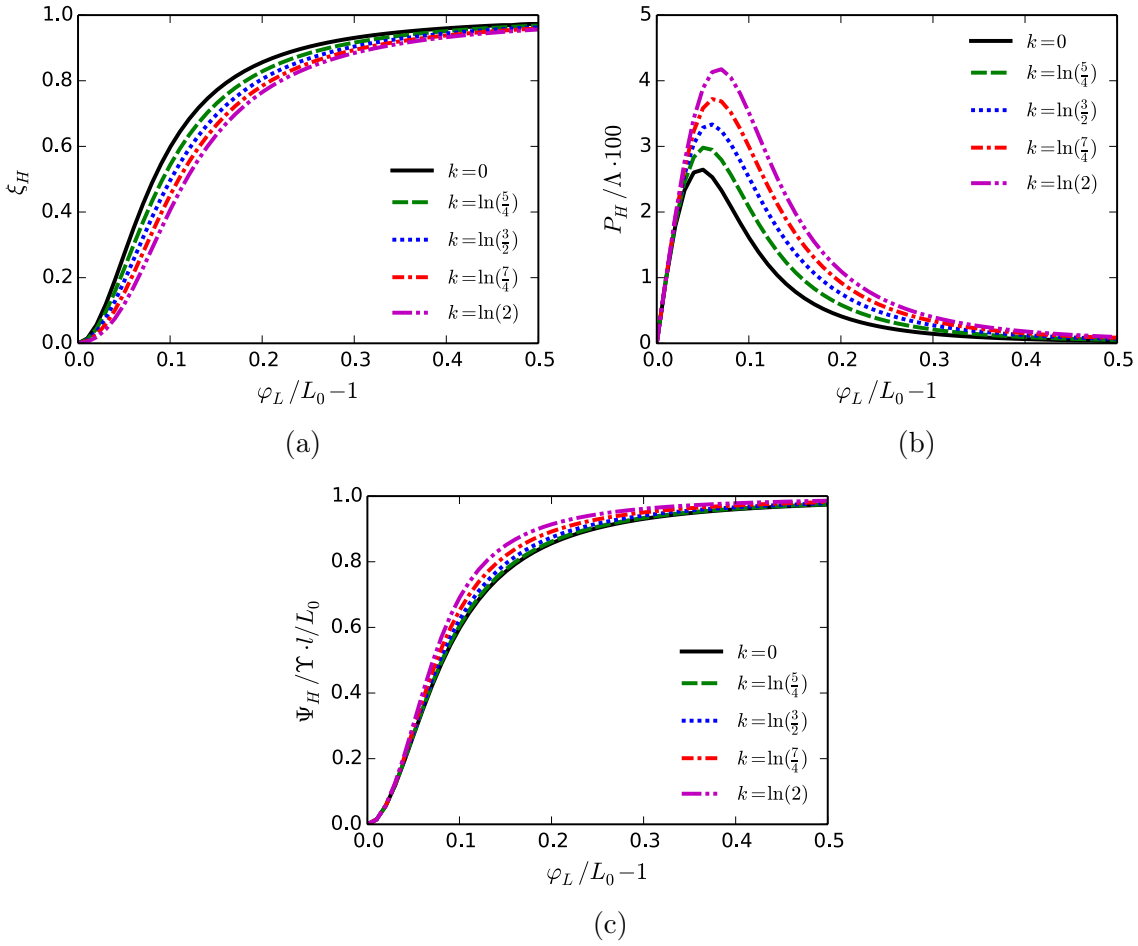

Fig. 1 Tensile deformation, homogeneous-state solutions, $l/L_0 = 10^{-3}$: (a) order parameter $\xi = D/l$, (b) normalized tensile stress, and (c) normalized total energy

4.4.2 Stress-Free State

As in Section 4.3.2, for a stress-free state $P = 0 \forall X \in [0, L_0]$. Boundary conditions on the order parameter $\xi(X)$ are prescribed as in Eq. 98:

$$\xi(0) = D(0)/l = 1, \qquad \xi(L_0) = 0. \tag{105}$$

The second of governing equations in Eq. 90, with Eq. 84, becomes the nonlinear second-order ordinary differential equation

$$\xi'' - \xi/l^2 + k[(\xi')^2 - \psi/(\Upsilon l)] = 0 \Rightarrow \xi'' = (\xi/l^2)(1 + k\xi). \tag{106}$$

Defining $\zeta = \xi'$ such that $\xi'' = \zeta \cdot \mathrm{d}\zeta/\mathrm{d}\xi$, this can be transformed into the nonhomogeneous first-order differential equation and corresponding general solution

$$\zeta \mathrm{d}\zeta = (\xi/l^2)(1 + k\xi)\mathrm{d}\xi \Rightarrow \zeta = \pm(\xi/l)\sqrt{1 + 2k\xi^2/3 + c_1/\xi^2}. \tag{107}$$

In this case, integration constant c_1 vanishes and the negative root applies. The second of Eq. 107 can be integrated to give the following implicit solution for $\xi(X)$, which is then evaluated via numerical quadrature:

$$\mathrm{d}\xi = -(\xi/l)\sqrt{1 + 2k\xi^2/3}\,\mathrm{d}X \Rightarrow X(\xi) = \int_1^{\xi} \frac{-l\mathrm{d}\alpha}{\alpha\sqrt{1 + 2k\alpha^2/3}}. \tag{108}$$

The null stress condition again results in $a(X) = 0 \forall \xi(X) \neq 1$ so that φ_0 and φ_L remain indeterminate. Total energy is the integral

$$\Psi(\xi) = \Psi_F = \int_0^{L_0} \Upsilon[(\xi')^2 l + \xi^2/l]\mathrm{d}X. \tag{109}$$

The total energy per unit cross-sectional area of the bar computed via Eq. 109 is shown in column 2 of Table 1, where $L_0 = 1$ for normalization. This energy Ψ_F increases slightly with increasing k, with the $k = 0$ solution identical to the stress-free solution from phase field theory.[43,64] A value of $\Psi_F/L_0^2 = \Upsilon$ corresponds to Griffith's theory of mode I brittle fracture, recalling that material property Υ is surface energy. Shown in Fig. 2 are profiles of ξ computed via Eq. 108, with a domain size of $L_0 = 10l$ and the same range of Weyl scaling factor k considered in Section 4.4.1. Regardless of k, the value of ξ drops off rapidly from its maximum at $X = 0$ with increasing X. Increasing k results in a small decrease in ξ for $X < L_0$, and an increase in $|\xi'|$ (i.e., a sharper fracture profile).

Table 1 Stress-free 1-D solutions for $l/L_0 = 0.1$: total energy

Weyl Scaling Factor	**Tension/Shear: $\Psi_F/(\Upsilon L_0^2)$**
$k = 0$	1.0091
$k = \ln\frac{5}{4}$	1.0100
$k = \ln\frac{3}{2}$	1.0117
$k = \ln\frac{7}{4}$	1.0138
$k = \ln 2$	1.0159

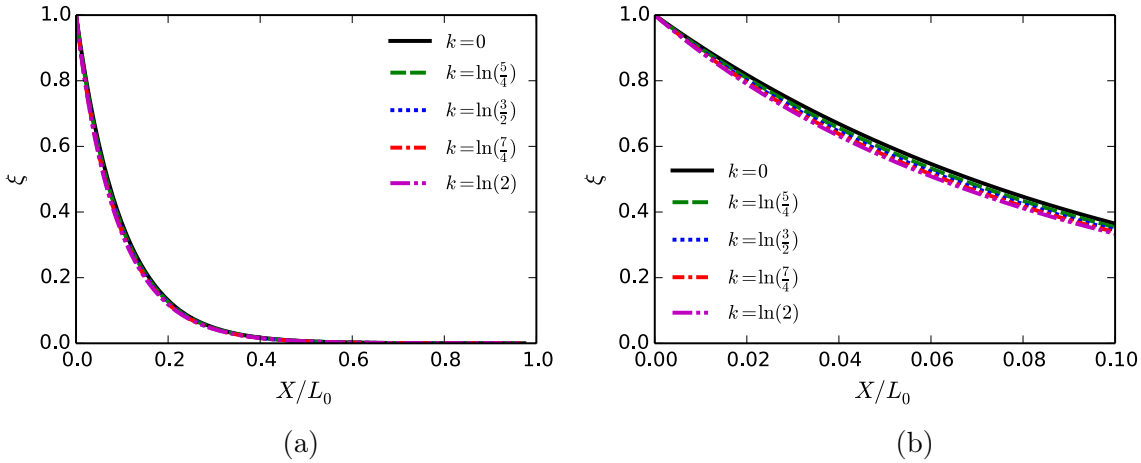

Fig. 2 Axial or shear stress-free solutions, $l/L_0 = 0.1$**: (a)** ξ**:** $0 \leq X \leq L_0$ **and (b)** ξ**:** $0 \leq X \leq 0.1L_0$

5. Physics of Slip

The second of 3 boundary value problems is considered in this section, involving simple shearing of a 2-D nonlinear elastic slab. Herein, a general free energy function is postulated, applicable for any 3-D deformation modes, and then specified to the present geometry and kinematics.

5.1 Problem Geometry and Kinematics

The material body is an elastic slab of length L_0 and infinite width and thickness. In 2 dimensions, the material manifold is specified as $\{\mathfrak{M} : X^1 \in [0, L_0], |X^2| \in \infty\}$. Regarding the third (out-of-plane) direction, plane strain conditions are imposed. The internal state vector is restricted as $\{D^A\} \to \{0, D^2, 0\}$. By construction, fields vary only with $X = X^1$ and $D = D^2$, and coordinates X^3, D^1, D^3 are superfluous. A Cartesian coordinate system suffices for $\{X\}$ so metric tensor $\boldsymbol{G}$ contains no dependence on X. Consistent with these protocols, the following reductions of definitions and identities of Section 2.1 hold:

$$\{X, Y\} = \{X^1, X^2\}, \qquad D = D^2; \tag{110}$$

$$\boldsymbol{G}(D) = \begin{bmatrix} G_{11}(D) & G_{12}(D) \\ G_{12}(D) & G_{22}(D) \end{bmatrix}, \quad G = G_{11}G_{22} - G_{12}^2; \tag{111}$$

$$\gamma_{ABC} = \tfrac{1}{2}(\partial_A G_{BC} + \partial_B G_{AC} - \partial_C G_{AB}) = 0, \qquad G^A = \tfrac{1}{2}\gamma^A_{BC} D^B D^C = 0; \tag{112}$$

$$N^A_B = \bar{\partial}_B G^A = 0 \Rightarrow \delta_A(\cdot) = \partial_A(\cdot); \tag{113}$$

$$\begin{aligned} C_{111} = & C_{122} = C_{212} = 0, \quad C_{222} = G'_{22}/2, \quad C_{112} = -G'_{11}/2, \\ & C_{121} = C_{211} = G'_{11}/2, \quad C_{221} = G'_{12}. \end{aligned} \tag{114}$$

The reference configuration space is locally Minkowskian. Invoking the Chern-Rund connection with vanishing nonlinear connection coefficients from Eq. 112,

$$\begin{aligned} & H^A_{BC} = K^A_{BC} = \Gamma^A_{BC} = \tfrac{1}{2} G^{AD}(\delta_C G_{BD} + \delta_B G_{CD} - \delta_D G_{BC}) = 0; \\ & V^A_{BC} = Y^A_{BC} = 0. \end{aligned} \tag{115}$$

For the current/deformed configuration of the slab, with deformed material manifold $\{\mathfrak{m} : x^1 \in [0, L], |x^2| \in \infty\}$, where L is the deformed length of the domain, spatial coordinates and metric components are of the Cartesian form

$$\{x, y\} = \{x^1, x^2\}, \quad d = d^2; \qquad g_{ab} = \delta_{ab}, \quad g = 1. \tag{116}$$

All spatial connection coefficients of Section 2.2—linear and nonlinear—then vanish identically.

Motions, deformations, and director gradients defined in Section 2.3 reduce as follows under simple shear, with $\varphi = \upsilon + Y$ and ϵ denoting deformation and strain in the shearing (Y) direction:

$$x = X, \quad y = \varphi(X, Y, D) = Y + \upsilon(X, D); \quad d = \vartheta(X, D); \quad D = D(X); \tag{117}$$

$$\begin{aligned} \boldsymbol{F}(X, D) &= \begin{bmatrix} \frac{\partial x(X)}{\partial X} & \frac{\partial x(X)}{\partial Y} \\ \frac{\partial \varphi(X,Y,D)}{\partial X} + \frac{\partial \varphi(X,Y,D)}{\partial X}\frac{\partial D(X)}{\partial X} & \frac{\partial \varphi(X,Y,D)}{\partial Y} \end{bmatrix} \\ &= \begin{bmatrix} 1 & 0 \\ \frac{\mathrm{d}\upsilon[X, D(X)]}{\mathrm{d}X} & 1 \end{bmatrix} = \begin{bmatrix} 1 & 0 \\ \epsilon(X, D) & 1 \end{bmatrix}; \end{aligned} \tag{118}$$

$$J(X, D) = \sqrt{g/G(D)} F^1_1(X, D) F^2_2(X, D) = [G(D)]^{-1/2} = J(D); \tag{119}$$

$$C_{11} = 1 + \epsilon^2, \quad C_{12} = C_{21} = \epsilon, \quad C_{22} = 1; \qquad \det \boldsymbol{C} = 1; \tag{120}$$

$$D^2_{|1} = \partial_1 D - N^2_1 + K^2_{12} D = \partial D / \partial X = D'. \tag{121}$$

The internal state variable D is physically identified with a slip discontinuity or slipped displacement. The defect associated with D could be a shear band in a (poly)crystalline metal,[66] a stacking fault in a crystal lattice,[19] or a mode II crack in a brittle solid.[43] It becomes useful to define a lattice shear strain measure a, deformation gradient $\bar{\boldsymbol{F}}$, deformation tensor $\bar{\boldsymbol{C}}$, and Jacobian determinant $\bar{J}$ as follows:

$$a = \epsilon \pm D' = \frac{\partial}{\partial X}(y - Y \pm D), \qquad \bar{\boldsymbol{F}}(X, D, D') = \begin{bmatrix} 1 & 0 \\ a(X, D, D') & 1 \end{bmatrix}; \quad (122)$$

$$\bar{C}_{11} = 1 + a^2, \quad \bar{C}_{12} = \bar{C}_{21} = a, \quad \bar{C}_{22} = 1; \qquad \bar{J} = \sqrt{\det(\bar{C}_{AB})}. \quad (123)$$

As in Section 4, introduced are a constant l with dimensions of length and a normalized order parameter $\xi \in [0, 1]$:

$$\xi = D/l, \qquad \xi' = D'/l; \qquad a = \epsilon \pm l\xi'. \quad (124)$$

Constant l will be identified as the value of shear slip-displacement at which the slab supports no shear stress. Letting k denote a constant depending on the material, a more specific form of the Minkowski metric in Eq. 110 is invoked:

$$\boldsymbol{G}(D) = \begin{bmatrix} \sqrt{G(D)} & 0 \\ 0 & \sqrt{G(D)} \end{bmatrix}; \quad G(\xi) = \exp(2k\xi) \Rightarrow \frac{G'}{2G} = \frac{G'_{11}}{G_{11}} = \frac{G'_{22}}{G_{22}} = \frac{k}{l}. \quad (125)$$

This can be viewed as a Weyl transformation or Weyl rescaling[48] of the Cartesian metric δ_{AB}. Also used later is the second component of the trace of Cartan's tensor of Eq. 114:

$$C^A_{2A} = G^{AB} C_{2AB} = \tfrac{1}{2}(G^{11}G'_{11} + G^{22}G'_{22} + 4G^{12}G'_{12}) = k/l. \quad (126)$$

The length of a referential line element in Eq. 14 and the corresponding volume form in Eq. 15 become

$$|\mathrm{d}\boldsymbol{X}|^2 = \exp\left(\frac{kD}{l}\right)(\mathrm{d}X \cdot \mathrm{d}X + \mathrm{d}Y \cdot \mathrm{d}Y), \quad d\Omega = \exp\left(\frac{kD}{l}\right)\mathrm{d}X \wedge \mathrm{d}Y. \quad (127)$$

For $\xi > 0$, expansion occurs when $k > 0$ and contraction when $k < 0$. Physical justification follows similar arguments as given in Section 4.1: shear fractures may result in dilatation as rough crack faces slide over one another,[67] while (full) dis-

locations or partial dislocations associated with shear bands or stacking faults may result in local dilatation due to nonlinear elastic and core effects.[68–70] Because G is not homogeneous of degree zero in D, the reference configuration space is not strictly of Finsler character, but is a pseudo-Finsler space,[16] and because G does not depend on X, this space may be further categorized as pseudo-Minkowskian.

5.2 Energy, Thermodynamic Forces, and Balance Laws

For a compressible neo-Hookean elastic solid with strain energy function W depending on lattice deformation tensor $\bar{\boldsymbol{C}}$, the following general form of total free energy density in Eq. 52 is assumed:

$$\psi(C_{AB}, D^A, D^A_{|B}, G_{AB}) = W[\bar{C}_{AB}(C_{AB}, D^A_{|B}), D^A] + f[D^A, D^A_{|B}, G_{AB}], \quad (128)$$

where function f accounts for surface energy. Specifically, extending prior phase field theory[43] to Finsler-geometric continuum mechanics, let μ and λ denote the usual isotropic elastic constants and

$$W = [\tfrac{1}{2}\mu(\bar{C}_{AB}\delta^{AB} - 3) - \mu \ln \bar{J} + \tfrac{1}{2}\lambda(\ln \bar{J})^2](1-\xi)^2, \quad (129)$$

$$f = (\Upsilon/l)(D^A D^B \delta_{AB}/l^2 + D^A_{|B}\delta_{AC}\delta^{BD}D^C_{|D}). \quad (130)$$

A stress tensor $\bar{\boldsymbol{P}}$ associated with W is

$$\bar{P}^A_a = \frac{\partial \psi}{\partial \bar{F}^a_A} = \frac{\partial W}{\partial \bar{F}^a_A} = [\mu \bar{F}^b_B \delta_{ab}\delta^{AB} + (\lambda \ln \bar{J} - \mu)\bar{F}^{-1}{}^A_a](1-\xi)^2. \quad (131)$$

For the present case of simple shear with Eqs. 120 and 123 now applied,

$$\partial\{\bar{F}^a_A[a(\epsilon, D')]\}/\partial F^b_B = (\partial a/\partial \epsilon)\delta^a_b \delta^A_B = \delta^a_b \delta^A_B \Rightarrow P^A_a = \bar{P}^A_a. \quad (132)$$

This identity, with $\bar{F}^2_1 = -(\bar{F}^{-1})^1_2 = a$ and $\bar{J} = 1$ in Eq. 131, results in the only nonzero stress components

$$P = P^1_2 = P^2_1 = \mu(1-\xi)^2 a. \quad (133)$$

The balance of angular momentum in Eq. 53 is verified as satisfied since, for the present problem,

$$\sigma^{ab} = \sigma^{ba} \Leftrightarrow P^2_1 = P^1_2 - \epsilon P^1_1 = P^1_2. \quad (134)$$

Derivations from Section 5.1 result in the following form of Eq. 128 that applies for the present example:

$$\begin{aligned}\psi = \psi(\epsilon, D, \partial D/\partial X) &= \psi(\partial \upsilon/\partial X, D, \partial D/\partial X) \\ &= W(\epsilon, D, \partial D/\partial X) + f(D, \partial D/\partial X).\end{aligned} \tag{135}$$

Written in terms of lattice shear strain and normalized order parameter, this becomes

$$\psi = \psi[a(\epsilon, \xi'), \xi, \xi'] = W[a(\epsilon, \xi'), \xi] + f(\xi, \xi'). \tag{136}$$

Adding f to the elastic strain energy W reduced under simple shear leads to

$$\psi = \tfrac{1}{2}\mu(1-\xi)^2 a^2 + \Upsilon\xi^2/l + \Upsilon l(\xi')^2. \tag{137}$$

The first term on the right side of Eq. 137 accounts for elastic strain energy degraded by damage associated with $\xi \in [0, 1]$, and the other 2 terms combine to account for surface energy associated with the particular class of shear defect (shear band, stacking fault, mode II crack, etc.) under consideration. This energy function contains no explicit dependence on G and is nearly identical to that of Eq. 84, differing only in the elastic constant (μ versus $\Lambda = \lambda + 2\mu$) and physical meanings of the lattice strain variable a, the order parameter ξ, and possible values of Υ and l.

Relevant (i.e., possibly nonzero) thermodynamic forces of Section 3 are then obtained by direct calculation as

$$P = P_2^1 = \frac{\partial \psi}{\partial \epsilon} = \frac{\partial W}{\partial a}\frac{\partial a(\epsilon, \xi')}{\partial \epsilon} = \mu(1-\xi)^2 a; \tag{138}$$

$$Q = Q_2 = \frac{\partial \psi}{\partial D} = \frac{1}{l}\frac{\partial \psi}{\partial \xi} = -\frac{\mu}{l}(1-\xi)a^2 + 2\frac{\Upsilon}{l^2}\xi = -\frac{Pa}{l(1-\xi)} + 2\frac{\Upsilon}{l^2}\xi; \tag{139}$$

$$Z = Z_2^1 = \frac{\partial \psi}{\partial D'} = \frac{1}{l}\frac{\partial \psi}{\partial \xi'} = 2\Upsilon\xi' + \frac{1}{l}\frac{\partial \psi}{\partial a}\frac{\partial a}{\partial \xi'} = 2\Upsilon\xi' - \mu(1-\xi)^2 a = 2\Upsilon\xi' - P. \tag{140}$$

Notice that Eq. 138 is consistent with Eq. 133. The linear momentum balance in Eqs. 59 and 64 becomes

$$\frac{\partial P(X, D)}{\partial X} + \frac{\partial P(X, D)}{\partial D}\frac{\partial D}{\partial X} + P\frac{G'(D)}{2G(D)}\frac{\partial D}{\partial X} = \frac{\mathrm{d}P}{\mathrm{d}X} + P\frac{G'}{2G}\frac{\mathrm{d}D}{\mathrm{d}X} = 0. \tag{141}$$

Micromomentum balances in Eqs. 60 and 65 become

$$\frac{\partial Z(X,D)}{\partial X}+\left[\frac{\partial Z(X,D)}{\partial D}+Z\frac{G'(D)}{2G(D)}+P\frac{\partial^2\upsilon(X,D)}{\partial D^2}\right]\frac{\partial D}{\partial X} - \frac{G'(D)}{G(D)}\psi(X,D)=Q(X,D). \tag{142}$$

Substituting from Eqs. 125, 126, and 138–140, these balance laws become, respectively,

$$\frac{\mathrm{d}P}{\mathrm{d}X}=-kP\frac{\mathrm{d}\xi}{\mathrm{d}X};\qquad P\left[\frac{a}{1-\xi}+\frac{\partial^2\upsilon}{\partial\xi^2}\xi'\right]+2\Upsilon l\xi''-2\frac{\Upsilon}{l}\xi=2k[\psi-\Upsilon l(\xi')^2]. \tag{143}$$

The relations in Eq. 143 are 2 coupled ordinary nonlinear differential equations wherein field variables P, a, ξ, $\upsilon=\varphi-Y$, and ψ depend ultimately on independent variable X.

Remark: Balance laws in Eqs. 90 and 143 are mathematically identical, but physically represent 2 different problems (i.e., tensile deformation and simple shear deformation), with P representing axial stress in the former and shear stress in the latter.

5.3 Problem Solutions: Riemannian Geometry

Considered first is a Riemannian referential configuration space (in fact, a Cartesian structure), with $k=0\rightarrow G=1=$ constant. As in Section 4.3, kinematics are still Finslerlian since φ can potentially depend explicitly on both D and X rather than just X. Balance laws in Eq. 143 reduce to

$$\frac{\mathrm{d}P}{\mathrm{d}X}=0;\qquad P\left[\frac{a}{1-\xi}+\frac{\partial^2\upsilon}{\partial\xi^2}\xi'\right]+2\Upsilon l\xi''-2\frac{\Upsilon}{l}\xi=0. \tag{144}$$

The first of Eq. 144 results immediately in spatially constant shear stress components:

$$P=P_0=\mu(1-\xi)^2a=\text{constant}. \tag{145}$$

The solution of the second balance equation requires more precise boundary conditions. Two problems corresponding to 2 different sets of boundary conditions are addressed: homogeneous damage of the deformed slab over $X\in[0,L]$ (i.e., microscopic shear fractures or slip bands $D=D^2$ evenly distributed along the finite

length of the slab) and localized damage corresponding to a globally stress-free deformed state (i.e., complete shear failure of the slab along a plane $X =$ constant).

5.3.1 Homogeneous Damage

For homogeneous damage, $\xi'(X) = 0 \forall X \in [0, L_0] \Rightarrow \xi(0) = \xi(L_0) = \xi_H$. Boundary conditions on shear displacement (or on φ along $Y = 0$) are prescribed as follows:

$$\upsilon(0, D) = \upsilon_0 = \pm D = \pm l\xi_H, \quad \upsilon(L_0, D) = \upsilon_L = a_H L_0 \pm l\xi_H. \tag{146}$$

Here, υ_L is the prescribed displacement of the deformed slab at $x = L$, with a_H and ξ_H constants. Evolving rigid body displacement (i.e., shear slip) at the end of the slab is quantified by υ_0. Equations 144 and 145 result in

$$P_0 = \mu(1 - \xi_H)^2 a_H, \qquad \xi_H = 1/[1 + 2\Upsilon/(\mu l a_H^2)]. \tag{147}$$

Given υ_L, Eqs. 146 and 147 can be solved simultaneously for the homogeneous damage field ξ_H, stress P_0, and lattice shear strain a_H. The problem kinematics are consistent with the separable decomposition of the motion φ into

$$\varphi[X, \xi(D), Y] = \upsilon(X, D) + Y = \chi(X) + Y \pm l\xi(D), \qquad F_1^2 = \mathrm{d}\varphi/\mathrm{d}X = \chi', \tag{148}$$

where for homogeneous damage and strain fields,

$$\varphi[X, \xi_H, Y] = a_H X + Y \pm l\xi_H, \qquad \chi = a_H X, \qquad F_1^2 = a_H. \tag{149}$$

The total energy of the slab per unit width in the Y-direction is obtained as

$$\begin{aligned} \Psi(\upsilon_L, \xi_H) = \Psi_H &= \int_0^{L_0} [\mu(1 - \xi_H)^2 a_H^2/2 + \Upsilon\xi_H^2/l]\mathrm{d}X \\ &= [\mu(1 - \xi_H)^2 a_H^2/2 + \Upsilon\xi_H^2/l] L_0. \end{aligned} \tag{150}$$

Remark: Letting $\varphi(X, Y, D) \to \varphi(X, Y) = \chi(X) + Y$ and modifying Eq. 146 to $\upsilon_0 = 0, \upsilon_L = a_H L_0$ recovers a description identical to a prior geometrically nonlinear phase field study.[43]

5.3.2 Stress-Free State

For a stress-free state, $P = P_0 = 0 \forall X \in [0, L_0]$. Boundary conditions on the order parameter $\xi(X)$ or internal state variable representing microshearing are prescribed as follows:

$$\xi(0) = D(0)/l = 1, \qquad \xi(L_0) = 0. \tag{151}$$

The second of governing equations in Eq. 144 becomes

$$\xi'' - \xi/l^2 = 0 \Rightarrow \xi(X) = c_1 \exp(X/l) + c_2 \exp(-X/l). \tag{152}$$

Constants c_1, c_2 are determined by boundary conditions in Eq. 151, leading to a particular analytical solution identical to that in the second of Eq. 99. The null stress condition results in $a(X) = 0 \forall \xi(X) \neq 1$; since lattice shear strain $a(X)$ and shear displacement $\upsilon_0 = \upsilon(0, D)$ are indeterminate where $\xi = 1$, the total shear displacement at the undamaged end of the slab, υ_L, is also indeterminate. Physically, this corresponds to rigidly displacing the bar, once disconnected from its fully localized and degraded site at $X = 0$, without altering its internal energy. Total energy per unit width is the integral

$$\Psi(\xi) = \Psi_F = \int_0^{L_0} \Upsilon[(\xi')^2 l + \xi^2/l] \mathrm{d}X. \tag{153}$$

Remark: Eq. 152 is a result identical to that of a phase field theory of shear failure[43]

.

5.4 Problem Solutions: Minkowskian Geometry

Considered now is a referential configuration space that is pseudo-Finslerian with $k \neq 0$ in Eq. 125. Even though the referential metric is pseudo-Minkowskian, deformation kinematics are again of Finsler nature. Balance laws in Eq. 143 apply; the first results in

$$\mathrm{d}P/P = -k\mathrm{d}\xi \Rightarrow P = P_0 \exp(-k\xi), \tag{154}$$

where P_0 is the constant shear stress corresponding to $k = 0$ and/or $\xi = 0$. The 2 problems considered in Sections 5.3.1 and 5.3.2 are revisited in the context of the pseudo-Minkowski metric in Eq. 125, recalling that $k > 0$ accounts for dilatation in the damaged or intensely sheared zone omitted in the Riemannian metrical representation of Section 5.3.

5.4.1 Homogeneous Damage

For homogeneous damage, $\xi'(X) = 0 \forall X \in [0, L_0] \Rightarrow \xi(0) = \xi(L_0) = \xi_H$. Boundary conditions on displacement $\upsilon = \varphi - Y$ are identical to Eq. 146:

$$\upsilon(0, D) = \upsilon_0 = \pm D = \pm l\xi_H, \quad \upsilon(L_0, D) = \upsilon_L = a_H L_0 \pm l\xi_H. \tag{155}$$

Equations 143 and 154 give

$$\begin{aligned} &P = P_0 \exp(-k\xi_H) = \mu(1 - \xi_H)^2 a_H = \text{constant}, \\ &\mu a_H^2(1 - \xi_H) - 2(\Upsilon/l)\xi_H = 2k\psi(a_H, \xi_H). \end{aligned} \tag{156}$$

Given υ_L, Eqs. 155 and 156 can be solved simultaneously for ξ_H, P_0, and a_H. Kinematics are consistent with separable decompositions in Eqs. 148 and 149. The total energy per unit width of the elastic slab is

$$\begin{aligned} \Psi(\upsilon_L, \xi_H) = \Psi_H &= \int_0^{L_0} [\mu(1 - \xi_H)^2 a_H^2/2 + \Upsilon\xi_H^2/l] \mathrm{d}X \\ &= [\mu(1 - \xi_H)^2 a_H^2/2 + \Upsilon\xi_H^2/l] L_0. \end{aligned} \tag{157}$$

Shown in Fig. 3 are $\xi = \xi_H$, $P = P_H$, and $\Psi = \Psi_H$ versus applied shear displacement, computed via Eqs. 156 and 157, where the positive choice $\varphi(X, Y, D) = \chi(X) + Y + D$ is applied in Eqs. 148 and 155. Representative material parameters are identical to those invoked in Section 4.4.1: $\mu = 10^9 \mathrm{N/m}^2$, $\Upsilon = 1\mathrm{N/m}$, $l = 10^{-9}\mathrm{m}$, $L_0 = 10^3 l$, and $0 \leq k \leq \ln 2$. Trends are similar to those depicted in Fig. 1. For fixed k, ξ increases monotonically with increasing shear displacement (Fig. 3a), shear stress P increases to a maximum and then decreases (Fig. 3b), and energy Ψ increases monotonically (Fig. 3c). As k increases, ξ tends to decrease for $0 < \upsilon_L/L_0 < 0.5$, while P and Ψ tend to increase. Effects of k are more pronounced in Fig. 3 than in Fig. 1, with the difference due to different elastic constants for shear and uniaxial tension (i.e., μ and $\Lambda = 3\mu$). Peak shear stress and applied displacement at which peak stress is attained both increase significantly with increasing k, implying an increase in shear strength and stability of the material commensurate with microscopic dilatation represented by $k > 0$. Again, increases in stress and energy correlate with a decrease in order parameter since both P and strain energy density W are affected by a multiplication factor of $(1 - \xi)^2$: see Eqs. 129 and 133. The contribution of the Finsler kinematic $l\xi_H$ term in Eq. 149—in other words, rigid

slip—is negligible for $l/L_0 \ll 1$, so the present Finsler solution with $k = 0$ and phase field theory[43] provide nearly identical results when microscopic dilatation is omitted.

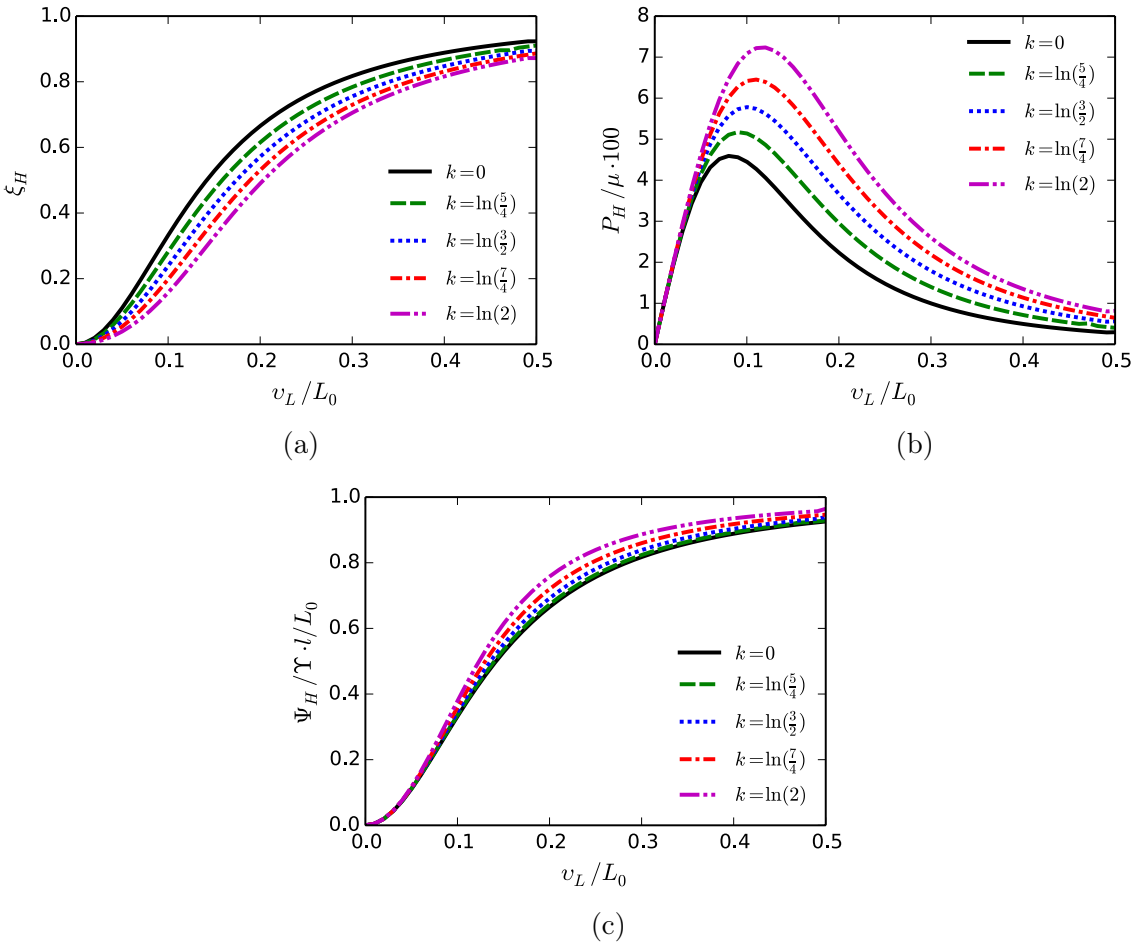

Fig. 3 Shear deformation, homogeneous-state solutions, $l/L_0 = 10^{-3}$: (a) order parameter $\xi = D/l$, (b) normalized shear stress, and (c) normalized total energy

5.4.2 Stress-Free State

Just as imposed in Section 5.3.2, let $P = 0 \forall X \in [0, L_0]$. Boundary conditions on $\xi(X)$ are prescribed as in Eq. 151:

$$\xi(0) = D(0)/l = 1, \qquad \xi(L_0) = 0. \tag{158}$$

The second of governing equations in Eq. 143, with the reduced form of energy density in Eq. 137, becomes the nonlinear second-order ordinary differential equation

$$\xi'' - \xi/l^2 + k[(\xi')^2 - \psi/(\Upsilon l)] = 0 \Rightarrow \xi'' = (\xi/l^2)(1 + k\xi). \tag{159}$$

Defining $\zeta = \xi'$ such that $\xi'' = \zeta \cdot \mathrm{d}\zeta/\mathrm{d}\xi$, this can be transformed into the nonhomogeneous first-order differential equation and corresponding general solution

$$\zeta \mathrm{d}\zeta = (\xi/l^2)(1 + k\xi)\mathrm{d}\xi \Rightarrow \zeta = \pm(\xi/l)\sqrt{1 + 2k\xi^2/3 + c_1/\xi^2}. \tag{160}$$

As in Section 4.4.2, the latter can be rewritten and then integrated to give

$$\mathrm{d}\xi = -(\xi/l)\sqrt{1 + 2k\xi^2/3}\,\mathrm{d}X \Rightarrow X(\xi) = \int_1^{\xi} \frac{-l\mathrm{d}\beta}{\beta\sqrt{1 + 2k\beta^2/3}}. \tag{161}$$

The null stress condition again results in $a(X) = 0 \forall \xi(X) \neq 1$ with v_0 and v_L indeterminate due to admissible rigid body motion. Total energy per unit width is the line integral

$$\Psi(\xi) = \Psi_F = \int_0^{L_0} \Upsilon[(\xi')^2 l + \xi^2/l]\mathrm{d}X. \tag{162}$$

Remark: Developments in Section 5.4.2 are mathematically identical to those of Section 4.4.2, but with different physical implications (i.e., shear failure versus tensile failure). Solutions depicted in Fig. 2 and Table 1 apply here, with identical mathematical trends to those discussed in Section 4.4.2, including close agreement of shear failure or mode II fracture energies among the present theory, phase field theory, and Griffith's theory. Physically, the pseudo-Finsler theory predicts that dilatation is associated with an increase in slip strength or crack sliding resistance as well as failure energy. Such predictions agree with physical observations.[67] In an intensely sheared zone, effects of microscopic friction or locking of asperities increase when the material dilates in such a zone. Recall from Section 5.1 that the dilatation here may be the result of heterogeneous (i.e., imperfect) microscopic fractures (as opposed to perfect cleavage), expansion of the material due to nonlinear elastic effects associated with defect cores (e.g., dislocation cores, point defects, and stacking faults[68]), and/or thermal expansion due to temperature rise in adiabatic shear.[66] It should be noted, however, that the present variational model does not explicitly monitor time-dependent dissipated energy associated with sliding friction or dislocation glide.

6. Physics of Cavitation

The final of 3 boundary value problems involves radial expansion of a spherical nonlinear elastic body. Cavitation (i.e., void or vacancy formation and growth) may occur uniformly throughout the domain and/or localized at or very near to the center of the sphere, depending on particular boundary conditions imposed in what follows. A general free energy function is postulated as in Section 5 and then specialized to the current geometry, but here curvilinear (specifically, spherical) coordinates are needed. This complicates the present analysis relative to those considered in Sections 4 and 5 that were tractable via Cartesian frames. The metric tensor necessarily depends on position and may also depend on the internal state vector; when the latter applies, a completely pseudo-Finslerian referential configuration space results.

6.1 Problem Geometry and Kinematics

The material body is an elastic sphere of radius R_0. The referential material manifold is specified as $\{\mathfrak{M} : R = X^1 \in [0, R_0], \Theta = X^2 \in [0, \pi], \Phi = X^3 \in (-\pi, \pi]\}$. By construction, spherical symmetry conditions are imposed so that solution field variables do not depend on angular coordinates Θ, Φ. The internal state vector is restricted to have a radial component only: $\{D^A\} \to \{D^1, 0, 0\}$. Metric tensor $\boldsymbol{G}$ necessarily depends on X and possibly depends on D. Consistent with these protocols, definitions and identities of Section 2.1 result in

$$\{R, \Theta, \Phi\} = \{X^1, X^2, X^3\}, \qquad \{D^1, D^2, D^3\} = \{D, 0, 0\}. \tag{163}$$

Denoting by $\bar{\boldsymbol{G}} = \bar{\boldsymbol{G}}(X)$ the usual metric tensor of Euclidean space in spherical coordinates[25,71] and $B = B(D)$ a differentiable scalar function of the internal state, the following separable form of the metric tensor $\boldsymbol{G}(X, D)$ is assumed:

$$\begin{aligned}\boldsymbol{G}(X, D) &= \bar{\boldsymbol{G}}(X)B(D) \\ &= \begin{bmatrix} \bar{G}_{11} & 0 & 0 \\ 0 & \bar{G}_{22}(X) & 0 \\ 0 & 0 & \bar{G}_{33}(X) \end{bmatrix} B(D) = \begin{bmatrix} 1 & 0 & 0 \\ 0 & R^2 & 0 \\ 0 & 0 & R^2 \sin^2\Theta \end{bmatrix} B(D);\end{aligned} \tag{164}$$

$$G = B^3 \bar{G} = B^3 R^4 \sin^2\Theta. \tag{165}$$

Let $\bar{\gamma}^A_{BC}$ denote Christoffel symbols of the second kind derived from $\bar{\boldsymbol{G}}$, and let γ^A_{BC} denote those derived from $\boldsymbol{G}$. From Eq. 6, these are equivalent:

$$\gamma^A_{BC} = G^{AD}\gamma_{BCD} = (B^{-1}\bar{G}^{AD})(B\bar{\gamma}_{BCD}) = \bar{\gamma}^A_{BC}. \tag{166}$$

Nonzero Christoffel symbols resulting from Eq. 164 are thus, with indices $(1,2,3) \leftrightarrow (R,\Theta,\Phi)$,[25,71]

$$\begin{aligned} &\gamma^\Theta_{R\Theta} = \gamma^\Phi_{R\Phi} = 1/R, \quad \gamma^R_{\Theta\Theta} = -R, \quad \gamma^\Phi_{\Theta\Phi} = \cot\Theta, \\ &\gamma^R_{\Phi\Phi} = -R\sin^2\Theta, \qquad \gamma^\Theta_{\Phi\Phi} = -\sin\Theta\cos\Theta. \end{aligned} \tag{167}$$

Since the only nonvanishing component of $\boldsymbol{D}$ is radial and since $\gamma^A_{RR} = 0$, the spray and nonlinear connection coefficients derived from it vanish identically for this problem:

$$G^A = \tfrac{1}{2}\gamma^A_{BC}D^BD^C = \tfrac{1}{2}\gamma^A_{RR}D\cdot D = 0, \qquad N^A_B = G^A_B = \bar{\partial}_B G^A = 0. \tag{168}$$

Denoting $B' = \partial B/\partial D^1 = \mathrm{d}B/\mathrm{d}D$, nonzero components of Cartan's tensor in Eq. 7 are

$$\begin{aligned} C_{111} = \tfrac{1}{2}B', \quad C_{122} = C_{212} = \tfrac{1}{2}B'R^2, \quad C_{133} = C_{313} = \tfrac{1}{2}B'R^2\sin^2\Theta, \\ C_{221} = -\tfrac{1}{2}B'R^2, \quad C_{331} = -\tfrac{1}{2}B'R^2\sin^2\Theta. \end{aligned} \tag{169}$$

The trace of Cartan's tensor in the radial direction will be used later:

$$C^A_{RA} = C^1_{11} + C^2_{12} + C^3_{13} = 3B'/(2B). \tag{170}$$

The reference configuration space is (pseudo)-Finslerian. Invoking the Chern-Rund connection with vanishing nonlinear connection coefficients from Eq. 168, horizontal coefficients are equal to Levi-Civita coefficients derived from $\bar{G}_{AB}$, while vertical coefficients vanish by definition of the Chern-Rund connection:

$$H^A_{BC} = K^A_{BC} = \Gamma^A_{BC} = \gamma^A_{BC}; \qquad V^A_{BC} = Y^A_{BC} = 0. \tag{171}$$

The spatial configuration manifold is specified as $\{\mathfrak{m} : r = x^1 \in [0, r_0], \theta = X^2 \in [0,\pi], \phi = x^3 \in (-\pi,\pi]\}$. Metric tensor $\boldsymbol{g}$ necessarily depends on x, but by construction does not depend on the internal state vector, whose spatial representation

$\boldsymbol{d}$ is presumed radial but does not further enter the problem at hand. Definitions and identities of Section 2.2 result in

$$\{r, \theta, \phi\} = \{x^1, x^2, x^3\}, \qquad \{d^1, d^2, d^3\} = \{d, 0, 0\}. \tag{172}$$

The following usual spherical form of a Riemannian metric tensor $\boldsymbol{g}(X)$ is assumed:

$$\boldsymbol{g}(x) = \begin{bmatrix} 1 & 0 & 0 \\ 0 & r^2 & 0 \\ 0 & 0 & r^2 \sin^2\theta \end{bmatrix}, \qquad g = r^4 \sin^2\theta. \tag{173}$$

Nonzero symbols resulting from Eq. 173 are, with indices $(1, 2, 3) \leftrightarrow (r, \theta, \phi)$,[25,71]

$$\begin{aligned} \gamma^{\theta}_{r\theta} = \gamma^{\phi}_{r\phi} = 1/r, \quad \gamma^{r}_{\theta\theta} = -r, \quad \gamma^{\phi}_{\theta\phi} = \cot\theta, \\ \gamma^{r}_{\phi\phi} = -r\sin^2\theta, \quad \gamma^{\theta}_{\phi\phi} = -\sin\theta\cos\theta. \end{aligned} \tag{174}$$

Since the metric is Riemannian as opposed to Finslerian (i.e., no dependence on $\{d\}$), Cartan's tensor vanishes, nonlinear connection coefficients from the spray vanish by arguments akin to Eq. 168, and the horizontal Chern-Rund coefficients coincide with Eq. 174:

$$c_{abc} = 0, \qquad n^a_b = 0, \qquad \Gamma^a_{bc} = \gamma^a_{bc}. \tag{175}$$

Analogously to Eq. 171, the following horizontal and vertical connection coefficents are imposed for gradients of basis vectors:

$$H^a_{bc} = K^a_{bc} = \Gamma^a_{bc} = \gamma^a_{bc}; \qquad V^a_{bc} = Y^a_{bc} = 0. \tag{176}$$

Motions, deformations, and director gradients defined in Section 2.3 reduce as follows under spherical expansion/contraction, with $\varphi = r$ denoting deformation in the radial (R) direction:

$$r = \varphi(R, D) = r(R, D), \quad \theta = \Theta, \quad \phi = \Phi; \quad d = \vartheta(R, D), \quad D = D(R); \tag{177}$$

$$\boldsymbol{F}(R, D) = \begin{bmatrix} \frac{\partial r(R,D)}{\partial R} + \frac{\partial r(R,D)}{\partial D}\frac{\partial D(R)}{\partial R} & 0 & 0 \\ 0 & \frac{\partial\theta}{\partial\Theta} & 0 \\ 0 & 0 & \frac{\partial\phi}{\partial\Phi} \end{bmatrix} = \begin{bmatrix} F^r_R(R, D) & 0 & 0 \\ 0 & 1 & 0 \\ 0 & 0 & 1 \end{bmatrix}; \tag{178}$$

$$J(R,D)=\sqrt{g(r,\theta)/G(R,\theta,D)}F_1^1(R,D)F_2^2F_3^3=[r^2F_R^r(R,D)]/(R^2B^{3/2}); \tag{179}$$

$$C_{11}=(F_R^r)^2,\quad C_{22}=r^2,\quad C_{33}=r^2\sin^2\theta,\quad C_{12}=C_{13}=C_{23}=0; \tag{180}$$

$$\det\boldsymbol{C}=J^2G; \tag{181}$$

$$D^1_{|1}=D^R_{|R}=\partial_R D-N^R_R+K^R_{RR}D=\partial D/\partial R=D'. \tag{182}$$

Internal state variable D is physically identified with radial microscopic opening in the material associated with cavitation. The defect associated with D could be, for example, a pore or void in a rock or metal or a site vacancy in a crystal lattice.[72,73] A lattice expansion measure a, deformation gradient $\bar{\boldsymbol{F}}$, deformation tensor $\bar{\boldsymbol{C}}$, and Jacobian determinant $\bar{J}$ are defined for future use as follows:

$$a(R,D,D')=F_R^r(R,D)-\frac{\mathrm{d}\vartheta[D(R)]}{\mathrm{d}D}\frac{\partial D(R)}{\partial R}=\frac{\partial}{\partial R}\{r(R,D)-\vartheta[D(R)]\}, \tag{183}$$

$$\bar{\boldsymbol{F}}(R,D,D')=\begin{bmatrix}a(R,D,D') & 0 & 0\\ 0 & 1 & 0\\ 0 & 0 & 1\end{bmatrix}; \tag{184}$$

$$\begin{aligned}\bar{C}_{AB}=\bar{F}^a_A g_{ab}\bar{F}^b_B;\qquad \bar{C}_{11}=a^2,\quad \bar{C}_{22}=r^2,\quad \bar{C}_{33}=r^2\sin^2\theta,\\ \bar{C}_{12}=\bar{C}_{13}=\bar{C}_{23}=0;\end{aligned} \tag{185}$$

$$\bar{J}=\sqrt{\det(\bar{C}_{AB})/\bar{G}}=\det\bar{\boldsymbol{F}}\sqrt{g/\bar{G}}=ar^2/R^2. \tag{186}$$

Local lattice expansion occurs at R for $a(R)>0$, contraction for $a(R)<0$. Here, $\vartheta[D(R)]$ is a continuous scalar function of its argument. As in Sections 4 and 5, constant l with dimensions of length and a normalized order parameter ξ are

$$\xi=D/l,\qquad \xi'=D'/l;\qquad a=\delta_R\varphi^r-\frac{\mathrm{d}\vartheta}{\mathrm{d}D}\frac{\mathrm{d}D}{\mathrm{d}R}=F_R^r-l\vartheta'\xi'. \tag{187}$$

The constant l will later be identified as the value of radial microdisplacement at which a material point within the sphere supports no radial stress. Letting k denote a constant depending on the material, a more specific form of the pseudo-Finsler metric in Eq. 164 is henceforth invoked:

$$\boldsymbol{G}(X,D)=\bar{\boldsymbol{G}}(X)B(D)=\bar{\boldsymbol{G}}(X)\exp(2k\xi/3),\quad B(D)=\exp[(2kD)/(3l)]; \tag{188}$$

$$B'/B = \bar{\partial}_1 G_{11}/G_{11} = \bar{\partial}_2 G_{22}/G_{22} = \bar{\partial}_3 G_{33}/G_{33} = 2k/(3l). \tag{189}$$

This can be viewed as a Weyl transformation or Weyl rescaling[48] of the spherical Euclidean metric $\bar{G}_{AB}$. The radial component of the trace of Cartan's tensor of Eq. 170 is

$$C^A_{RA} = 3B'/(2B) = k/l. \tag{190}$$

The length of a referential line element in Eq. 14 and the corresponding volume form in Eq. 15 become

$$\begin{aligned} |\mathrm{d}\boldsymbol{X}|^2 &= \exp(2k\xi/3)(\mathrm{d}R \cdot \mathrm{d}R + R^2 \mathrm{d}\Theta \cdot \mathrm{d}\Theta + R^2 \sin^2\Theta \mathrm{d}\Phi \cdot \mathrm{d}\Phi), \\ d\Omega &= \exp(k\xi/3) R^2 \sin\Theta \mathrm{d}R \wedge \mathrm{d}\Theta \wedge \mathrm{d}\Phi. \end{aligned} \tag{191}$$

For $\xi > 0$, expansion occurs when $k > 0$ and contraction when $k < 0$. Physical justification is obvious for the former: cavitation and void growth are associated with expansion. The latter condition would apply for collapse of existing pores, for example. Because G is not homogeneous of degree zero in D, the reference configuration space is a pseudo-Finsler space.[16]

6.2 Energy, Thermodynamic Forces, and Balance Laws

Analogoulsy to that considered in Section 5.2, a compressible neo-Hookean strain energy function W depending on lattice deformation tensor $\bar{\boldsymbol{C}}$ is assumed to enter ψ of Eq. 52:

$$\psi(C_{AB}, D^A, D^A_{|B}, G_{AB}) = W[\bar{C}_{AB}(C_{AB}, D^A_{|B}), D^A, \bar{G}_{AB}] + f[D^A, D^A_{|B}, \bar{G}_{AB}], \tag{192}$$

where function f accounts for intrinsic energy of spherical defects, such as surface energy of a void or cavity. With μ and λ denoting the usual isotropic elastic constants,

$$W = [\{\tfrac{1}{2}\mu(\bar{C}_{AB}\bar{G}^{AB} - 3) - \mu \ln \bar{J} + \tfrac{1}{2}\lambda(\ln \bar{J})^2](1-\xi)^2, \tag{193}$$

$$f = (\Upsilon/l)(D^A \bar{G}_{AB} D^B/l^2 + D^A_{|B} \bar{G}_{AC} \bar{G}^{BD} D^C_{|D}). \tag{194}$$

A generally nonsymmetric stress tensor $\bar{\boldsymbol{P}}$ associated with W is

$$\bar{P}^A_a = \frac{\partial W}{\partial \bar{F}^a_A} = \frac{\partial \psi}{\partial \bar{F}^a_A} = [\mu \bar{F}^b_B g_{ab} \bar{G}^{AB} + (\lambda \ln \bar{J} - \mu)\bar{F}^{-1\,A}_{\quad a}](1-\xi)^2. \tag{195}$$

Since $\bar{\boldsymbol{G}}(X)$ does not depend on D, $S^{AB} = 0$ follows from the prescription in Eq. 192.

For the present case of spherical symmetry with Eqs. 180 and 185 now applied,

$$\partial\{\bar{F}^a_A[a(F^r_R, D')]\}/\partial F^b_B = (\partial a/\partial F^r_R)\delta^a_b\delta^A_B = \delta^a_b\delta^A_B \Rightarrow P^A_a = \bar{P}^A_a. \tag{196}$$

This identity, with $\bar{F}^1_1 = a$, $\bar{F}^2_2 = \bar{F}^3_3 = 1$ and $\bar{J}$ defined in Eq. 186, produces the only nonzero stress components

$$\begin{aligned} P = P^1_1 = P^R_r &= \frac{(1-\xi)^2}{a}[\mu(a^2-1) + \lambda \ln \bar{J}], \\ P^2_2 = P^\Theta_\theta = P^3_3 = P^\Phi_\phi &= (1-\xi)^2\left[\mu\left(\frac{r^2-R^2}{R^2}\right) + \lambda \ln \bar{J}\right]. \end{aligned} \tag{197}$$

The balance of angular momentum in Eq. 53 is trivially satisfied since $\boldsymbol{F}$ and $\boldsymbol{g}$ are of diagonal form and all shear stresses vanish.

Using derivations from Section 6.1, the following form of Eq. 192 applies henceforth:

$$\begin{aligned} \psi = \psi(F^r_R, D, \partial D/\partial R) &= W[a(F^r_R, \xi'), r, \xi] + f(\xi, \xi') \\ &= (1-\xi)^2 W_0[a(F^r_R, \xi'), r] + f(\xi, \xi'). \end{aligned} \tag{198}$$

Adding f to the elastic strain energy W reduced under spherical deformation leads to the following reduced form of total free energy density ψ:

$$\begin{aligned} \psi(a, r, \xi, \xi') &= (1-\xi)^2 W_0(a, r) + \Upsilon\xi^2/l + \Upsilon l(\xi')^2 \\ &= (1-\xi)^2\{\tfrac{1}{2}\mu(a^2 + 2r^2/R^2 - 3) - \mu \ln(ar^2/R^2) \\ &\qquad + \tfrac{1}{2}\lambda[\ln(ar^2/R^2)]^2\} + \Upsilon[\xi^2/l + l(\xi')^2]. \end{aligned} \tag{199}$$

Nonzero thermodynamic forces are then computed as follows, with stress components consistent with Eq. 197:

$$\begin{aligned} P &= \frac{(1-\xi)^2}{a}[\mu(a^2-1) + \lambda \ln(ar^2/R^2)], \\ T &= \frac{R}{2r}(P^\Theta_\theta + P^\Phi_\phi) = \frac{R(1-\xi)^2}{r}[\mu(r^2/R^2 - 1) + \lambda \ln(ar^2/R^2)]; \end{aligned} \tag{200}$$

$$Q = Q_R = \frac{\partial \psi}{\partial D} = \frac{1}{l}\frac{\partial \psi}{\partial \xi} = 2\frac{\Upsilon}{l^2}\xi - \frac{2(1-\xi)}{l}W_0; \tag{201}$$

$$Z = Z_R^R = \frac{\partial \psi}{\partial D_{|1}^1} = \frac{1}{l}\frac{\partial \psi}{\partial \xi'} = \frac{1}{l}\frac{\partial f}{\partial \xi'} + \frac{(1-\xi)^2}{l}\frac{\partial W_0[a(F_R^r, \xi'), r]}{\partial a}\frac{\partial a}{\partial \xi'} = 2\Upsilon\xi' - P. \tag{202}$$

The following scalar function will also be invoked later, where ψ is the function in Eq. 199:

$$\begin{aligned} \iota(a, r, \xi, \xi') &= [2B/(3B')]G^{AB}\bar{\partial}_1 G_{AB}\psi(a, r, \xi, \xi') = 2\psi(a, r, \xi, \xi') \\ &= 2(1-\xi)^2 W_0(a, r) + 2\Upsilon[\xi^2/l + l(\xi')^2]. \end{aligned} \tag{203}$$

Momentum balances specific to the present problem are derived as follows. Thelinear momentum balance in Eq. 59 yields the three equations ($a = 1, 2, 3 = r, \theta, \phi$):

$$\partial_A P_a^A + \bar{\partial}_B P_a^A \partial_A D^B + P_a^B \gamma_{AB}^A - P_c^A \gamma_{ba}^c F_A^b + P_a^A C_{BC}^C \partial_A D^B = 0. \tag{204}$$

For $a = 2, 3$, since $P_\theta^\Theta = P_\phi^\Phi$ from Eq. 197, and $\theta = \Theta, \phi = \Phi$ from spherically symmetric deformation, these reduce to the two trivially satisfied equations

$$P_\theta^\Theta \gamma_{A\Theta}^A - P_\phi^\Phi \gamma_{\phi\theta}^\phi F_\Phi^\phi = P_\theta^\Theta \cot\Theta - P_\phi^\Phi \cot\theta = 0, \qquad P_c^A \gamma_{b\phi}^c F_A^b = 0. \tag{205}$$

A nontrivial linear momentum balance remains for the radial direction $a = 1 = r$ in Eq. 204:

$$\partial_R P + \frac{\partial P}{\partial D}\frac{\partial D}{\partial R} + \frac{2}{R}P - \frac{1}{r}(P_\theta^\Theta + P_\phi^\Phi) + P C_{RA}^A \frac{\partial D}{\partial R} = 0. \tag{206}$$

The only nontrivial component of the micromomentum balance in Eq. 60 is for the radial direction, $C = 1 = R$:

$$\frac{\partial Z}{\partial R} + \frac{2}{R}Z + \left(\frac{\partial Z}{\partial D} + P\frac{\partial^2 \varphi}{\partial D^2}\right)\frac{\partial D}{\partial R} + \frac{3B'}{2B}\left(Z\frac{\partial D}{\partial R} - \iota\right) = Q. \tag{207}$$

Substituting from Eqs. 190 and 200 leads to, with P and T radial and transverse stress components, the following reduced form of Eq. 206:

$$\frac{\mathrm{d}P}{\mathrm{d}R} + \frac{2}{R}(P - T) = -kP\frac{\mathrm{d}\xi}{\mathrm{d}R}. \tag{208}$$

Substituting from Eqs. 190, 201, 202, and 203 and multiplying Eq. 207 by $\frac{l}{2}$ gives

$$\begin{aligned}\Upsilon l\xi'' + \frac{2\Upsilon l}{R}\xi' - \frac{\Upsilon}{l}\xi - \frac{l}{2}\left(\frac{\mathrm{d}P}{\mathrm{d}R} - \frac{P}{l}\frac{\partial^2 r}{\partial \xi^2}\xi'\right) + (1-\xi)W_0 \\ = k\left[\frac{l}{2}P\xi' + (1-\xi)^2 W_0 + \frac{\Upsilon}{l}\xi^2\right].\end{aligned} \tag{209}$$

Relations in Eqs. 208 and 209 are 2 coupled nonlinear ordinary differential equations wherein field variables P, T, a, r, ξ, and W_0 depend ultimately on independent variable R.

6.3 Problem Solutions: Riemannian Geometry

Considered first is a Riemannian referential configuration space with $k = 0 \rightarrow B = 1 = \text{constant} \Rightarrow \boldsymbol{G}(X, D) \rightarrow \bar{\boldsymbol{G}}(X)$. As in Sections 4.3 and 5.3, kinematics are still Finslerian since φ can potentially depend on both D and R rather than just R. Balance laws in Eqs. 208 and 209 reduce to

$$\begin{aligned}&\frac{\mathrm{d}P}{\mathrm{d}R} = \frac{2}{R}(T-P); \\ &\Upsilon l\xi'' + \frac{2\Upsilon l}{R}\xi' - \frac{\Upsilon}{l}\xi + (1-\xi)W_0 + \frac{P}{2}\left[\frac{2l}{R}\left(1-\frac{T}{P}\right) + \frac{\partial^2 r}{\partial \xi^2}\xi'\right] = 0.\end{aligned} \tag{210}$$

Unlike the problem considered in Section 4.3, the first of Eq. 210 does not necessarily lead to spatially uniform stress fields. Instead, $\frac{\mathrm{d}P}{\mathrm{d}R} = 0$ occurs only for the case of $P = T$, corresponding to a spherical and hydrostatic stress state:

$$\mathrm{d}P/\mathrm{d}R = 0 \Leftrightarrow T = P = P_r^R = (R/r)P_\theta^\Theta = (R/r)P_\phi^\Phi = P_0 = \text{constant}. \tag{211}$$

From Eq. 197, conditions in Eq. 211 require homogeneous lattice strain of the form $a = r/R$ and/or complete cavitation $\xi(R) = 1 \forall R \in \mathfrak{M}$ since

$$P = T + (1-\xi)^2 \mu[(a - r/R) - (1/a - R/r)]. \tag{212}$$

Solutions of Eq. 210 require more precise boundary conditions. Two problems corresponding to 2 different sets of boundary conditions are addressed: homogeneous damage of the deformed sphere over $R \in [0, R_0]$ (i.e., microscopic voids or vacancies $D = D^R = D^1$ evenly distributed within the volume, in conjunction with possible opening at the origin) and localized cavitation corresponding to a globally stress-free deformed state (i.e., complete cavitation $\xi \rightarrow 1$ as $R \rightarrow 0$).

6.3.1 Homogeneous Damage

For homogeneous damage, $\xi'(R) = 0 \forall R \in [0, R_0] \Rightarrow \xi(0) = \xi(R_0) = \xi_H$. Boundary conditions on radial displacement $r = \varphi$ are prescribed as follows:

$$r(0, D) = \varphi_0 = D = l\xi_H, \quad r(R_0, D) = \varphi_R = a_H R_0 + l\xi_H. \tag{213}$$

Here, φ_R is the prescribed outer radius of the deformed sphere, with $a_H = a(R_0)$ and ξ_H constants. The evolving radius of the discrete cavity at the origin can be interpreted as φ_0. The problem kinematics, with $\xi' = 0$ and $\vartheta = D$, are consistent with the separable decomposition of the motion φ into

$$\varphi[R, \xi(D)] = \chi(R) + \vartheta(D) = \chi(R) + l\xi(D), \qquad F = F_R^r = \partial\varphi/\partial R = \chi' = a. \tag{214}$$

Equations 197 and 210 result in

$$\begin{aligned} P(R) &= \frac{(1-\xi_H)^2}{a}[\mu(a^2-1) + \lambda \ln(ar^2/R^2)]; \\ \frac{\Upsilon}{l}\xi_H &= (1-\xi_H)W_0[a(R), r(R)] + P\left[\frac{l}{R}\left(1 - \frac{T}{P}\right)\right]. \end{aligned} \tag{215}$$

Given φ_R, then it follows that Eq. 212, the second of Eq. 213, and Eq. 215 evaluated at $r(R_0) = \varphi_R$ can be solved simultaneously for the homogeneous damage field ξ_H, stresses $P_H = P(R_0)$ and $T_H = T(R_0)$, and the lattice strain $a(R_0) = a_H$. Then, with ξ_H so determined, Eqs. 214 and 215 can be solved simultaneously along $R < R_0$ to determine the distribution of deformations, stresses, and resulting energy density inside the sphere. The total energy of the elastic sphere is obtained via the volume integral

$$\Psi(\varphi_R, \xi_H) = \Psi_H = 4\pi \int_0^{R_0} \{(1-\xi_H)^2 W_0[a(R), r(R)] + \Upsilon\xi_H^2/l\} R^2 \mathrm{d}R. \tag{216}$$

Remark: Letting $\varphi(r, D) \to \varphi(R) = \chi(R)$ and modifying Eq. 213 to $\varphi_0 = 0, \varphi_R = a_H R_0$ recovers a classical rather than Finslerian description of deformation kinematics in which micromotion D does not contribute to macromotion φ. In such a case, the homogeneous solution for deformation is $a = r/R = a_H = \varphi_R/R_0 =$ constant, with $P = T = P_0 =$ constant and ξ_H determined by simultaneous solution of Eq. 215. Bifurcation[74] to a cavitated state at the origin is not addressed by this classical solution.

6.3.2 Stress-Free State

For a stress-free spherical manifold $\mathfrak{M}$, $P = T = 0 \forall R \in [0, R_0]$. Particular boundary conditions on the order parameter $\xi(R)$ or internal state variable representing microdisplacement are prescribed somewhat analogously to Eqs. 98 and 151 as

$$\xi(\varepsilon_0 R_0) = D(\varepsilon_0 R_0)/l = 1 - \varepsilon_0, \qquad \xi(R_0) = 0. \tag{217}$$

As demonstrated in Eq. 218, the general analytical solution for ξ is singular at $R = 0$; therefore, the solution space is restricted to the domain $\epsilon_0 \leq R/R_0 \leq 1$, where $\epsilon_0 \ll 1$ is a small parameter. Linear momentum balance corresponding to the first of Eq. 210 is trivially satisfied. Noting that W_0 vanishes for a stress-free state, the second of the governing equations in 210 becomes the homogeneous nonlinear second-order ordinary differential equation for the field $\xi = \xi(R)$ with corresponding general solution

$$\xi'' + (2/R)\xi' - \xi/l^2 = 0 \Rightarrow \xi(R) = (1/R)[c_1 \exp(R/l) + c_2 \exp(-R/l)]. \tag{218}$$

With particular boundary conditions of Eq. 217 imposed, the complete solution for $R_0 = 1$ is

$$\xi(R) = \frac{\varepsilon_0}{R} \frac{(1 - \varepsilon_0) \exp[-(R + \varepsilon_0)/l]}{\exp[2(1 - \epsilon_0)/l] - 1} [\exp(2R/l) - \exp(2/l)]. \tag{219}$$

Remark: Unlike the problems considered in Sections 4.3.2 and 5.3.2, the displacement condition at the outer (inner) boundary R_0 ($\varepsilon_0 R_0$) is not arbitrary, since vanishing stress in Eq. 197 requires $a = r/R = 1 \forall R : \xi \neq 1$. The boundary conditions in Eq. 217 thus imply $r(R_0) = R_0$ in this case. Since the radial order parameter gradient need not vanish, consistency with the nonlinear elastic constitutive model requires $\vartheta = 0$ in the first of Eq. 183 since $a = \partial_R r = 1$ for this example.

6.4 Problem Solutions: Finslerian Geometry

Considered now is the general scenario wherein the referential configuration space is pseudo-Finslerian with $k \neq 0$ in Eq. 188. Here the referential metric is pseudo-Finslerian, and deformation kinematics are of Finsler character because motion function $r = \varphi(R, D)$ can potentially depend on D as well as R. Balance laws

in Eqs. 208 and 209 apply in full; substituting the first into the second results in

$$\Upsilon l\xi'' + \frac{2\Upsilon l}{R}\xi' - \frac{\Upsilon}{l}(1+k\xi)\xi + \frac{P}{2}\left[\frac{2l}{R}\left(1-\frac{T}{P}\right) + \frac{\partial^2 r}{\partial \xi^2}\xi'\right] + (1-\xi)[1-k(1-\xi)]W_0 = 0. \tag{220}$$

Solutions again require specification of boundary conditions. The same 2 problems considered in Sections 6.3.1 and 6.3.2 are now revisited in the context of the pseudo-Finsler metric in Eq. 188, recalling that $k > 0$ accounts for microscopic dilatation in the cavitated or porous zone omitted in the Riemannian metrical representation of Section 6.3.

6.4.1 Homogeneous Damage

For homogeneous damage, $\xi'(R) = 0 \forall R \in [0, R_0] \Rightarrow \xi(0) = \xi(R_0) = \xi_H$. Boundary conditions on displacement are identical to Eq. 213:

$$r(0, D) = \varphi_0 = D = l\xi_H, \quad r(R_0, D) = \varphi_R = a_H R_0 + l\xi_H, \tag{221}$$

where φ_R is the prescribed outer radius of the deformed sphere, with a_H and ξ_H constants, and with φ_0 the cavity radius at the core of the body. Equations in 214 still apply. Equations 197 and 220 result in

$$P(R) = \frac{(1-\xi_H)^2}{a}[\mu(a^2-1) + \lambda \ln(ar^2/R^2)], \tag{222}$$

$$\frac{\Upsilon}{l}(1+k\xi_H)\xi_H = \frac{Pl}{R}\left(1-\frac{T}{P}\right) + (1-\xi_H)[1-k(1-\xi_H)]W_0[a(R), r(R)]. \tag{223}$$

Given displacement boundary condition φ_R in Eq. 221, the solution procedure is analogous to that described in Section 6.3.1 (albeit here with $k \neq 0$), and the total energy of the cavitated elastic sphere is again obtained via the volume integral in Eq. 216.

Shown in Fig. 4 are $\xi = \xi_H$, $P(R_0) = P_H$, and $\psi(R_0)$ versus applied radial displacement, computed via Eqs. 222 and 223. Material parameters are identical to those invoked in Section 4.4.1: $\mu = 10^9 \mathrm{N/m}^2$, $\Upsilon = 1\mathrm{N/m}$, $l = 10^{-9}\mathrm{m}$, $R_0 = 10^3 l$, and $0 \leq k \leq \ln 2$. Trends are similar to those of Fig. 1 and Fig. 3: for fixed k, ξ increases monotonically with increasing radial displacement (Fig. 4a), radial stress P increases to a maximum and then decreases (Fig. 4b), and local energy density

ψ at the surface of the sphere increases monotonically (Fig. 4c). As k increases, ξ tends to decrease for $1.0 < \varphi_R/R_0 < 1.5$, while P and ψ tend to increase. Variations in fields with displacement are more abrupt in the present spherical solutions than in the 1-D solutions of Sections 4.4.1 and 5.4.1. Peak radial stress and applied displacement at which peak stress is attained both increase significantly with increasing k, implying an increase in cavitation resistance and stability of the material commensurate with microscopic dilatation represented by $k > 0$. Increases in stress and energy correlate with a decrease in order parameter since both P and strain energy density W are affected by a multiplication factor of $(1-\xi)^2$ in Eqs. 193 and 197.

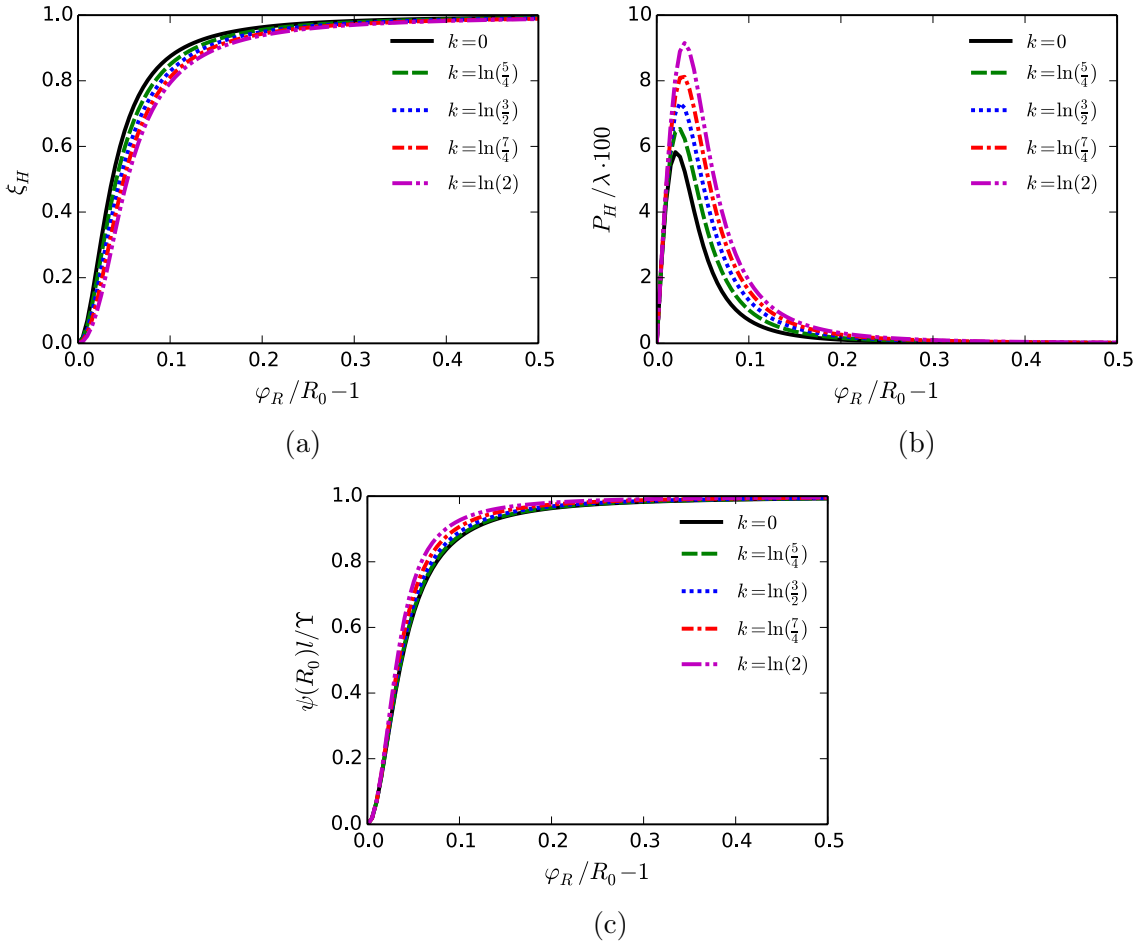

Fig. 4 Spherical deformation, homogeneous-state solutions, $l/R_0 = 10^{-3}$: (a) order parameter $\xi = D/l$, (b) normalized radial stress, and (c) normalized boundary energy density

Remark: Letting $\varphi(r, D) \to \varphi(R) = \chi(R)$ and changing Eq. 221 to $\varphi_0 = 0, \varphi_R = a_H R_0$ recovers a classical description of kinematics in which micromotion D does not contribute to macro-motion φ. Then the homogeneous solution for deformation is $a = r/R = a_H = \varphi_R/R_0 =$ constant, with $P = T = P_0 =$ constant and ξ_H determined by the simultaneous solution of Eqs. 222 and 223. Again, this homogeneous solution does not address the bifurcation problem of cavitation as often studied in classical nonlinear elasticity,[74] nor does it address the possible instability associated with breaking of spherical symmetry.[75]

6.4.2 Stress-Free State

As in Section 6.3.2, for a stress-free state $P = 0 \forall R \in [0, R_0]$. Boundary conditions on the order parameter $\xi(R)$ are as in Eq. 217:

$$\xi(\varepsilon_0 R_0) = D(\varepsilon_0 R_0)/l = 1 - \varepsilon_0, \qquad \xi(R_0) = 0. \tag{224}$$

The linear momentum balance in Eq. 208 is trivially satisfied, and $\vartheta = 0$ as remarked in Section 6.3.2. The micromomentum balance in Eq. 220 becomes, with $W_0 = 0$, the following homogeneous nonlinear second-order ordinary differential equation for state variable field $\xi = \xi(R)$:

$$\xi'' + (2/R)\xi' - (1/l^2)(1 + k\xi)\xi = 0. \tag{225}$$

This equation has no known general analytical solution for $k \neq 0$. Therefore, solutions are obtained numerically via a second-order accurate finite difference scheme with an iterative evaluation of the nonlinear $k\xi$ term. Shown in Fig. 5 are profiles of ξ computed via such a scheme, with $\varepsilon_0 = 0.01$, $R_0 = 10l$ and the same range of Weyl scaling factor k considered in Section 4.4.1. Regardless of k, ξ decreases rapidly from its maximum at $R = \varepsilon_0 R_0$ with increasing R to the imposed boundary value $\xi(R_0) = 0$. Increasing k provides no apparent change in ξ for $R < R_0$ for spherical solutions in Fig. 5, in contrast to 1-D Cartesian solutions shown in Fig. 2. The total energy per unit surface area of the sphere is shown in column 2 of Table 2, where $R_0 = 1$ for normalization. This energy Ψ_F increases slightly with increasing k, similarly to trends observed for uniaxial tension and simple shear deformations in column 2 of Table 1.

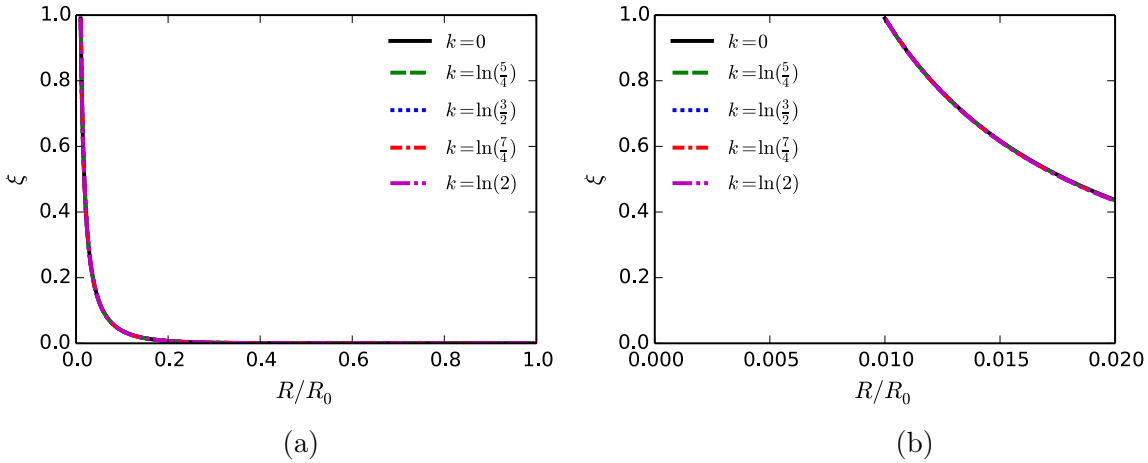

Fig. 5 Spherical stress-free solutions, $l/R_0 = 0.1$**: (a)** ξ**:** $0 \leq R \leq R_0$ **and (b)** ξ**:** $0 \leq R \leq 0.02R_0$

Table 2 Stress-free spherical solutions for $l/L_0 = 0.1$**: total energy**

Weyl Scaling Factor	**Cavitation:** $\Psi_F/(4\pi R_0^2 \Upsilon) \cdot 10^3$
$k = 0$	1.1077
$k = \ln \frac{5}{4}$	1.1080
$k = \ln \frac{3}{2}$	1.1082
$k = \ln \frac{7}{4}$	1.1083
$k = \ln 2$	1.1085

7. Conclusion

A new theory, in general considering a deformable vector bundle of pseudo-Finsler character, has been posited, wherein the internal state vector of pseudo-Finsler space is associated with microdeformation of a material with internal structure. The general objective has been a physically meaningful theory that is more descriptive and more predictive than existing models, without ad hoc equations or numerous fitting parameters. Rather, the focus has been development of general, and at times more sophisticated, governing equations instead of rudimentary additions to existing model frameworks. The specifically proposed problem solutions offer new physical insight into coupling of microscopic dilatation—captured herein by a conformal transformation of the metric tensor—with fracture or slip in solids. It has been demonstrated how the present results can encompass known phase field solu-

tions when a Riemannian rather than pseudo-Finslerian metric is used and how such results compare favorably with those of Griffith's fracture mechanics. Furthermore, the model predicts an increase in peak strength, displacement at instability, and failure energy with increasing microscopic dilatation in the intensely damaged or localized shearing zone, in agreement with physical observation. The general theory is capable of addressing more diverse physical phenomena in condensed matter depending on differently assumed forms of the fundamental tensor (e.g., anisotropy or directional rescaling) and different sets of connection coefficients, as may be demonstrated in future work.

Further remarks on how the proposed Finsler-geometric framework may be extended and applied to problems of relevance in the context of prior and ongoing work by the author in topical areas of defect mechanics, structural transformations, and shock physics are in order. Regarding defect mechanics, the internal state vector could be enlarged to account for various components of defect density tensors (e.g., dislocations, disclinations, and/or point defects[38,39,72,76–78]). Phase field descriptions of deformation twinning[60,79] and its competition with fracture[43,80,81] could be modeled via identification of state vector components with twinning shear as well as local crack opening. Solid-solid phase transformations such as stress-induced amorphization[82,83] are a natural application of the present framework, which, as has been shown, encompasses and extends existing phase field theory[83] to account for additional physics such as microdilatation. Particular crystalline materials of interest that display twins, slip/shear bands, and fractures include magnesium,[60,80] sapphire or corundum,[80,84] and boron carbide.[46,82,83] For shock physics applications, consideration of alternative nonlinear elastic potentials[85–87] as well as inertial effects becomes important. Explicit time dependence of field quantities has been omitted in this report, which has focused, for simplicity/brevity of presentation, on an incremental, quasi-static variational model. Formulation of a complete dynamic Finsler-geometric continuum theory with dissipation poses no foreseeable difficulties. For example, kinetic equations extending the Ginzburg-Landau[88] or Allen-Cahn[89] formalism for state vector evolution to the present Finsler modeling framework should be readily possible.

8. References

1. Randers G. On an asymmetrical metric in the four-space of general relativity. Physical Review. 1941;59:195–199.

2. Ikeda S. On the theory of fields in Finsler spaces. Journal of Mathematical Physics. 1981;22:1215–1218.

3. Brandt H. Differential geometry of spacetime tangent bundle. International Journal of Theoretical Physics. 1992;31:575–580.

4. Kerner E. Extended intertial frames and Lorentz transformations. II. Journal of Mathematical Physics. 1976;17:1797–1807.

5. Ohta SI, Sturm KT. Non-contraction of heat flow on Minkowski spaces. Archive for Rational Mechanics and Analysis. 2012;204:917–944.

6. Saczuk J. On the role of the Finsler geometry in the theory of elasto-plasticity. Reports on Mathematical Physics. 1997;39:1–17.

7. Finsler P. Uber kurven und flachen in allgemeiner raumen [dissertation]. [Gottingen (Germany)]: University of Gottingen; 1918.

8. Cartan E. Les espaces de finsler. Paris (France): Hermann; 1934.

9. Chern SS. Local equivalence and Euclidean connections in Finsler spaces. Scientific Reports of National Tsing Hua University Series A. 1948;5:95–121.

10. Rund H. The differential geometry of Finsler spaces. Berlin (Germany): Springer-Verlag; 1959.

11. Bao D, Chern SS, Shen Z. An introduction to Riemann-Finsler geometry. New York (NY): Springer-Verlag; 2000.

12. Bejancu A, Farran H. Geometry of pseudo-finsler submanifolds. Dordrecht (The Netherlands): Kluwer; 2000.

13. Chern SS, Shen Z. Riemann-Finsler geometry. Singapore (Singapore): World Scientific; 2005.

14. Bejancu A. Finsler geometry and applications. New York (NY): Ellis Horwood; 1990.

15. Vargas J, Torr D. Finslerian structures: the Cartan-Clifton method of the moving frame. Journal of Mathematical Physics. 1993;34:4898–4913.

16. Minguzzi E. The connections of pseudo-Finsler spaces. International Journal of Geometric Methods in Modern Physics. 2014;11:1460025.

17. Amari S. A theory of deformations and stresses of ferromagnetic substances by Finsler geometry. In: RAAG Memoirs; Vol. 3; Kondo K, editor. Tokyo (Japan): 1962; p. 257–278.

18. Toupin R, Rivlin R. Dimensional changes in crystals caused by dislocations. Journal of Mathematical Physics. 1960;1:8–15.

19. Clayton J. Nonlinear mechanics of crystals. Dordrecht (The Netherlands): Springer; 2011.

20. Le K, Stumpf H. On the determination of the crystal reference in nonlinear continuum theory of dislocations. Proceedings of the Royal Society of London A. 1996;452:359–371.

21. Wenzelburger J. A kinematic model for continuous distributions of dislocations. Journal of Geometry and Physics. 1998;24:334–352.

22. Clayton J, Bammann D, McDowell D. Anholonomic configuration spaces and metric tensors in finite strain elastoplasticity. International Journal of Non-Linear Mechanics. 2004;39:1039–1049.

23. Clayton J. On anholonomic deformation, geometry, and differentiation. Mathematics and Mechanics of Solids. 2012;17:702–735.

24. Clayton J. Aspects of differential geometry and tensor calculus in anholonomic configuration space. In: Oberwolfach Reports; Vol. 9; Greuel GM, editor. European Mathematical Society; 2012; p. 898–900.

25. Clayton J. Differential geometry and kinematics of continua. Singapore (Singapore): World Scientific; 2014.

26. Kondo K. Non-holonomic foundations of the theory of plasticity and yielding. In: RAAG Memoirs; Vol. 1; Kondo K, editor. Tokyo (Japan): 1955; p. 522–562.

27. Kondo K. Non-Riemannian and Finslerian approaches to the theory of yielding. International Journal of Engineering Science. 1963;1:71–88.

28. Kröner E. Interrelations Between Various Branches of Continuum Mechanics. In: Mechanics of Generalized Continua; Kröner E, editor. Berlin (Germany): Springer; 1968; p. 330–340.

29. Eringen A. Tensor Analysis. In: Continuum Physics; Vol. I; Eringen A, editor. New York (NY): Academic Press; 1971; p. 1–155.

30. Mindlin R. Microstructure in linear elasticity. Archive for Rational Mechanics and Analysis. 1964;16:51–78.

31. Ikeda S. A geometrical construction of the physical interaction field and its application to the rheological deformation field. Tensor, N.S. 1972;24:60–68.

32. Ikeda S. A physico-geometrical consideration on the theory of directors in the continuum mechanics of oriented media. Tensor, N.S. 1973;27:361–368.

33. Stumpf H, Saczuk J. A generalized model of oriented continuum with defects. Zeitschrift für Angewandte Mathematik und Mechanik (ZAMM). 2000;80:147–169.

34. Yajima T, Nagahama H. Finsler geometry of seismic ray path in anisotropic media. Proceedings of the Royal Society of London A. 2009;465:1763–1777.

35. Clayton J. On Finsler geometry and applications in mechanics: review and new perspectives. Advances in Mathematical Physics. 2015;828475.

36. Noll W. Materially uniform simple bodies with inhomogeneities. Archive for Rational Mechanics and Analysis. 1967;27:1–32.

37. Wang CC. On the geometric structures of simple bodies, a mathematical foundation for the theory of continuous distributions of dislocations. Archive for Rational Mechanics and Analysis. 1967;27:33–94.

38. Clayton J, Bammann D, McDowell D. A geometric framework for the kinematics of crystals with defects. Philosophical Magazine. 2005;85:3983–4010.

39. Clayton J. Defects in nonlinear elastic crystals: differential geometry, finite kinematics, and second-order analytical solutions. Zeitschrift für Angewandte Mathematik und Mechanik (ZAMM). 2015;95:476–510.

40. Steinmann P. Geometrical foundations of continuum mechanics. Berlin (Germany): Springer; 2015.

41. Saczuk J. Finslerian Foundations of Solid Mechanics. Gdansk (Poland): Polskiej Akademii Nauk; 1996.

42. Friedrich M, Schmidt B. An analysis of crystal cleavage in the passage from atomistic models to continuum theory. Archive for Rational Mechanics and Analysis. 2015;217:263–308.

43. Clayton J, Knap J. Nonlinear phase field theory for fracture and twinning with analysis of simple shear. Philosophical Magazine. 2015;95:2661–2696.

44. Brace W, Paulding B, Scholz C. Dilatancy in the fracture of crystalline rocks. Journal of Geophysical Research. 1966;71:3939–3953.

45. Clayton J. Deformation, fracture, and fragmentation in brittle geologic solids. International Journal of Fracture. 2010;163:151–172.

46. Clayton J, Tonge A. A nonlinear anisotropic elastic-inelastic constitutive model for polycrystalline ceramics and minerals with application to boron carbide. International Journal of Solids and Structures. 2015;64–65:191–207.

47. Clayton J. An alternative three-term decomposition for single crystal deformation motivated by non-linear elastic dislocation solutions. Quarterly Journal of Mechanics and Applied Mathematics. 2014;67:127–158.

48. Weyl H. Space-Time-Matter. 4th ed. New York (NY): Dover; 1952.

49. Canuto V, Adams P, Hsieh SH, Tsiang E. Scale-covariant theory of gravitation and astrophysical applications. Physical Review D. 1977;16:1643–1663.

50. Ozakin A, Yavari A. A geometric theory of thermal stresses. Journal of Mathematical Physics. 2010;51:032902.

51. Clayton J, McDowell D. A multiscale multiplicative decomposition for elastoplasticity of polycrystals. International Journal of Plasticity. 2003;19:1401–1444.

52. Clayton J. Dynamic plasticity and fracture in high density polycrystals: constitutive modeling and numerical simulation. Journal of the Mechanics and Physics of Solids. 2005;53:261–301.

53. Clayton J. Modeling dynamic plasticity and spall fracture in high density polycrystalline alloys. International Journal of Solids and Structures. 2005;42:4613–4640.

54. Kohn R. The relaxation of a double-well energy. Continuum Mechanics and Thermodynamics. 1991;3:193–236.

55. Bhattacharya K. Microstructure of martensite: why it forms and how it gives rise to the shape-memory effect. New York (NY): Oxford University Press; 2003.

56. Rund H. A divergence theorem for Finsler metrics. Monatshefte fur Mathematik. 1975;79:233-252.

57. Grinfeld M. Thermodynamic methods in the theory of heterogeneous systems. Sussex (United Kingdom): Longman Scientific and Technical; 1991.

58. Grinfeld P. Introduction to tensor analysis and the calculus of moving surfaces. New York (NY): Springer; 2013.

59. Truesdell C, Toupin R. The Classical Field Theories. In: Handbuch der Physik; Vol. III/1; Flugge S, editor. Berlin (Germany): Springer-Verlag; 1960; p. 226–793.

60. Clayton J, Knap J. A phase field model of deformation twinning: nonlinear theory and numerical simulations. Physica D: Nonlinear Phenomena. 2011;240:841–858.

61. Capriz G. Continua with microstructure. New York (NY): Springer; 1989.

62. Clayton J, Chung P. An atomistic-to-continuum framework for nonlinear crystal mechanics based on asymptotic homogenization. Journal of the Mechanics and Physics of Solids. 2006;54:1604–1639.

63. E W, Ming P. Cauchy-Born rule and the stability of crystalline solids: static problems. Archive for Rational Mechanics and Analysis. 2007;183:241–297.

64. Borden M, Verhoosel C, Scott M, Hughes T, Landis C. A phase-field description of dynamic brittle fracture. Computer Methods in Applied Mechanics and Engineering. 2012;217:77–95.

65. Steinmann P, Carol I. A framework for geometrically nonlinear continuum damage mechanics. International Journal of Engineering Science. 1998;36:1793–1814.

66. Wright T. The physics and mathematics of adiabatic shear bands. Cambridge (United Kingdom): Cambridge University Press; 2002.

67. Curran D, Seaman L, Cooper T, Shockey D. Micromechanical model for comminution and granular flow of brittle material under high strain rate application to penetration of ceramic targets. International Journal of Impact Engineering. 1993;13:53–83.

68. Holder J, Granato A. Thermodynamic properties of solids containing defects. Physical Review. 1969;182:729–741.

69. Clayton J, Bammann D. Finite deformations and internal forces in elastic-plastic crystals: interpretations from nonlinear elasticity and anharmonic lattice statics. Journal of Engineering Materials and Technology. 2009;131:041201.

70. Clayton J, Hartley C, McDowell D. The missing term in the decomposition of finite deformation. International Journal of Plasticity. 2014;52:51–76.

71. Ogden R. Non-linear elastic deformations. Chichester (United Kingdom): Ellis Horwood; 1984.

72. Clayton J. A non-linear model for elastic dielectric crystals with mobile vacancies. International Journal of Non-Linear Mechanics. 2009;44:675–688.

73. Clayton J. Modeling nonlinear electromechanical behavior of shocked silicon carbide. Journal of Applied Physics. 2010;107:013520.

74. Ball J. Discontinuous equilibrium solutions and cavitation in nonlinear elasticity. Philosophical Transactions of the Royal Society of London A. 1982;306:557–611.

75. Abeyaratne H, Hou H. On the occurrence of the cavitation instability relative to the asymmetric instability under symmetry dead-loading conditions. Quarterly Journal of Mechanics and Applied Mathematics. 1991;44:429–449.

76. Clayton J, McDowell D, Bammann D. A multiscale gradient theory for elasto-viscoplasticity of single crystals. International Journal of Engineering Science. 2004;42:427–457.

77. Clayton J, McDowell D, Bammann D. Modeling dislocations and disclinations with finite micropolar elastoplasticity. International Journal of Plasticity. 2006;22:210–256.

78. Clayton J, Chung P, Grinfeld M, Nothwang W. Kinematics, electromechanics, and kinetics of dielectric and piezoelectric crystals with lattice defects. International Journal of Engineering Science. 2008;46:10–30.

79. Clayton J, Knap J. Phase field modeling of twinning in indentation of transparent single crystals. Modelling and Simulation in Materials Science and Engineering. 2011;19:085005.

80. Clayton J, Knap J. Phase field analysis of fracture induced twinning in single crystals. Acta Materialia. 2013;61:5341–5353.

81. Clayton J, Knap J. Phase field modeling of coupled fracture and twinning in single crystals and polycrystals. Computer Methods in Applied Mechanics and Engineering. 2016;in press.

82. Clayton J. Towards a nonlinear elastic representation of finite compression and instability of boron carbide ceramic. Philosophical Magazine. 2012;92:2860–2893.

83. Clayton J. Phase field theory and analysis of pressure-shear induced amorphization and failure in boron carbide ceramic. AIMS Materials Science. 2014;1:143–158.

84. Clayton J. A continuum description of nonlinear elasticity, slip and twinning, with application to sapphire. Proceedings of the Royal Society A. 2009;465:307–334.

85. Clayton J. Nonlinear Eulerian thermoelasticity for anisotropic crystals. Journal of the Mechanics and Physics of Solids. 2013;61:1983–2014.

86. Clayton J. Analysis of shock compression of strong single crystals with logarithmic thermoelastic-plastic theory. International Journal of Engineering Science. 2014;79:1–20.

87. Clayton J. Crystal thermoelasticity at extreme loading rates and pressures: analysis of higher-order energy potentials. Extreme Mechanics Letters. 2015;3:113–122.

88. Levitas V, Levin V, Zingerman K, Freiman E. Displacive phase transitions at large strains: phase-field theory and simulations. Physical Review Letters. 2009;103:025702.

89. Allen S, Cahn J. A microscopic theory for antiphase boundary motion and its application to antiphase domain coarsening. Acta Metallurgica. 1979;27:1085–1095.

INTENTIONALLY LEFT BLANK.

1 (PDF)	DEFENSE TECHNICAL INFORMATION CTR DTIC OCA
2 (PDF)	DIRECTOR US ARMY RESEARCH LAB RDRL CIO LL IMAL HRA MAIL & RECORDS MGMT
1 (PDF)	GOVT PRINTG OFC A MALHOTRA
1 (PDF)	CALIFORNIA INST TECHNOLOGY K BHATTACHARYA
1 (PDF)	DREXEL UNIVERSITY DEPT MATHEMATICS P GRINFELD
1 (PDF)	GEORGIA INST TECHNOLOGY D MCDOWELL
1 (PDF)	MISSISSIPPI STATE UNIVERSITY CENTER ADVANCED VEHICULAR SYSTEMS D BAMMANN
1 (PDF)	NEW YORK UNIVERSITY COURANT INST MATH SCI R KOHN

ABERDEEN PROVING GROUND

20 (PDF) DIR USARL
RDRL CIH C
J KNAP
RDRL WM
B FORCH
S KARNA
J MCCAULEY
J ZABINSKI
RDRL WML B
B RICE
RDRL WMM B
G GAZONAS
RDRL WMP
S SCHOENFELD
RDRL WMP B
S SATAPATHY
M SCHEIDLER
A SOKOLOW
RDRL WMP C
R BECKER
T BJERKE
J CLAYTON
M GREENFIELD
R LEAVY
J LLOYD
S SEGLETES
A TONGE
C WILLIAMS